Review of Recent Status of Coded Aperture X-ray Monitors for Beam Size Measurement

John Flanagan

IBIC2018
Shanghai
2018.9.12

Outline

- Review of Principles:
  - Wide-aperture imaging in x-ray astronomy
  - Principles of Coded Aperture Imaging
  - Other x-ray imaging approaches at accelerators
- Experiences at:
  - Diamond Light Source
  - CesrTA
  - ATF2
  - SuperKEKB
- Summary and Prospects

- Discovery of extra-solar x-ray sources in 1962 via non-imaging, rocket-born detector. →Birth of x-ray astronomy

R. Giacconiet al., "Evidence for x Rays from Sources Outside the Solar System," Phys. Rev. Lett. 9, 439, Dec. 1962

Einstein satellite (1978-1982)

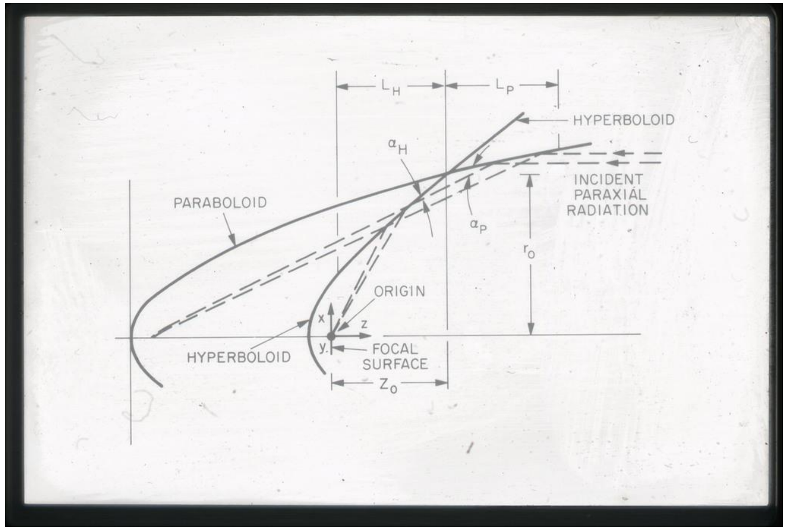

https://www.cfa.harvard.edu/about/history/images/einstein/slides/index.html

- "The first imaging, extra-solar X-ray telescope
- **A set of 4 Wolter type 1 nested mirrors focused X-rays up to 8 keV in energy**.
- 1 degree field of view
- Both an imaging proportional counter (IPC) and micro-channel plate detector (HRI) were included."

https://heasarc.gsfc.nasa.gov/docs/einstein/heao2.html

See also: R. Giacconi et al, ApJ, vol 230, p 540, 1979

https://www.cfa.harvard.edu/about/history/einstein/index.html

XMM-Newton satellite (1999-now)

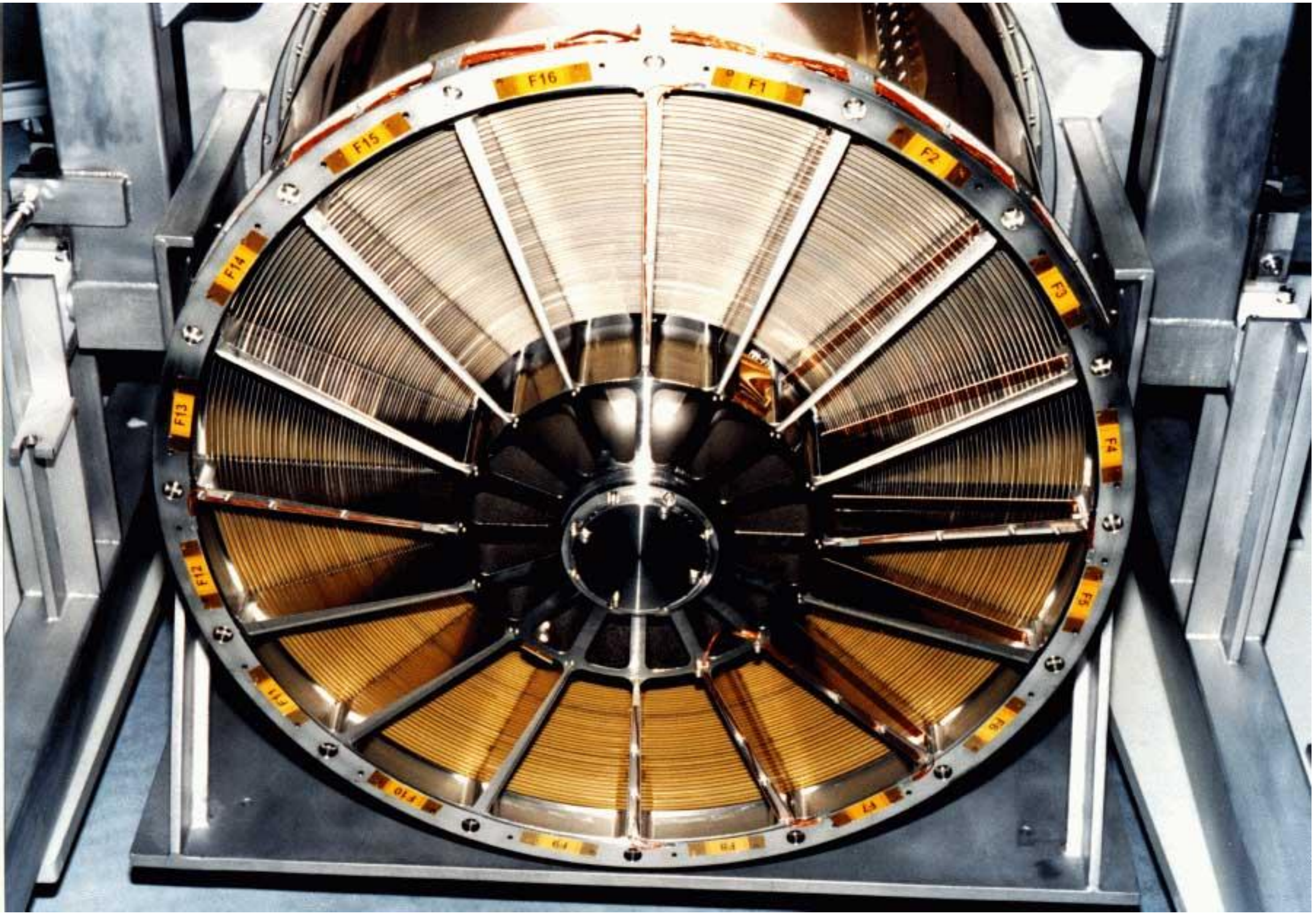

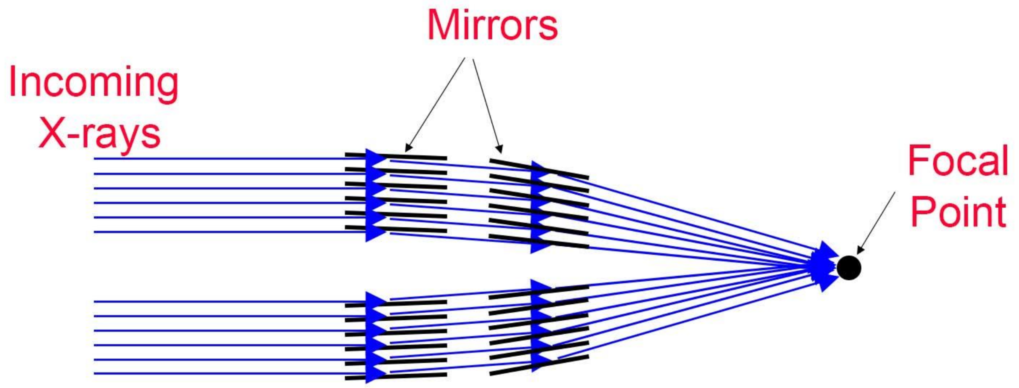

Note: For accelerators, machining such a set of mirrors would seem difficult due to:

- Size constraints, unless perhaps one can get sufficient distance from source and sufficiently large opening angle of synchrotron fan.
- Maximum intensity of SR fan is in center, where mirror coverage is lacking.

https://imagine.gsfc.nasa.gov/science/toolbox/xray_telescopes1.html

Multi-layer mirrors

- Current approaches include multi-layer mirrors, using constructive interference from alternating high- and low-index of refraction materials to enhance light-collection efficiency over certain wavelength ranges.

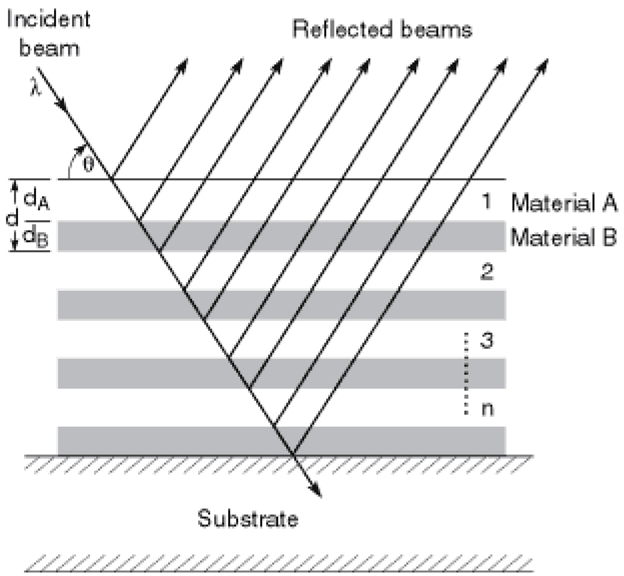

Figure from: A. Thompson et al., “Handbook of X-ray Optics,” LBNL PUB-490 Rev. 3, p. 4-2 2009.
http://xdb.lbl.gov/xdb-new.pdf

NuSTAR: Nested mirrors, 3-79 keV
(10 meters between mirrors and detectors)

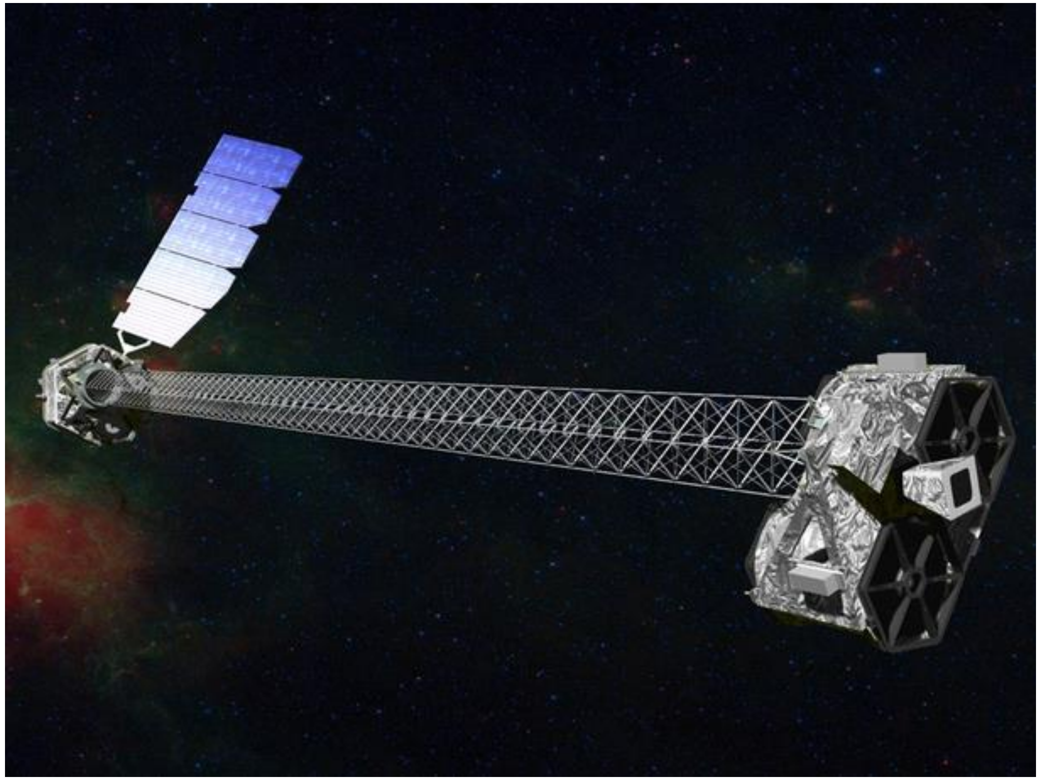

“NuSTAR implements a conical approximation to the Wolter-I design which consists of 133 concentric mirror shells coated with Pt/SiC and W/Si multilayers. The optics operate in the energy range 3 - 79 keV.”
https://www.nustar.caltech.edu/page/instrumentation

Figure: https://www.nustar.caltech.edu/image/nustarconcept02

Principles of Coded Aperture Imaging

- Technique developed by x-ray astronomers, gamma-ray astronomers and others, using a mask to modulate incoming light. Resulting image must be deconvolved through mask response (including diffraction and spectral width) to reconstruct object.
- X-ray astronomer R. Dicke proposed to use multiple pinholes to increase photon-collection efficiency.
  - He proposed randomly-spaced pinholes.
  - Produces complicated detector image, that can be recovered by deconvolution by cross-correlation with original mask image.

R.H. Dicke, Astrophys. Journ., 153, L101, (1968).

Principles of Coded Aperture Imaging

- In principle, any set of multiple apertures can be considered a "coded aperture."
  - Even Fresnel zone plates have been proposed for use – if detuned so as not to act like a lens, then an FZP provides a uniformly distributed set of aperture widths and spacings, for uniform spatial resolution over a range of sizes.

L. Mertz and N. Young, Proceedings of the International Conference on Optical Instruments and Techniques (Chapman and Hall, London, 1961), p. 305

- Special case: Uniformly Redundant Arrays (URAs)
  - Pseudo-random arrangement of apertures, with nice mathematical property that auto-correlation is a delta function, so reconstruction has no side-lobe artifacts, as tend to occur for truly random arrays (and FZPs).

E.E. Fenimore and T.M. Cannon, Appl. Optics, V17, No. 3, p. 337 (1978).

Coded Aperture X-ray & Gamma-ray Telescopes

→Wide Aperture (~50%)
→Wide angular and spectral acceptance
→Short distance between optics and detector

- **ProtoMIRAX: URA, 5-200 keV**

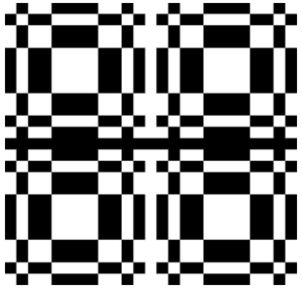

2x2 repeating pattern

J.Braga, "Development of the balloon-borne hard X-ray experiment protoMIRAX," talk at 29th Texas Symposium on Relativistic Astrophysics, Cape Town, South Africa, 3-8 Dec. 2017

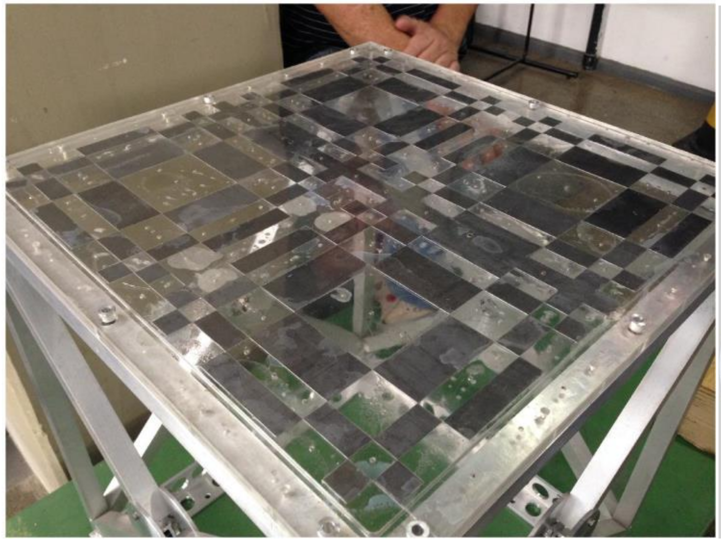

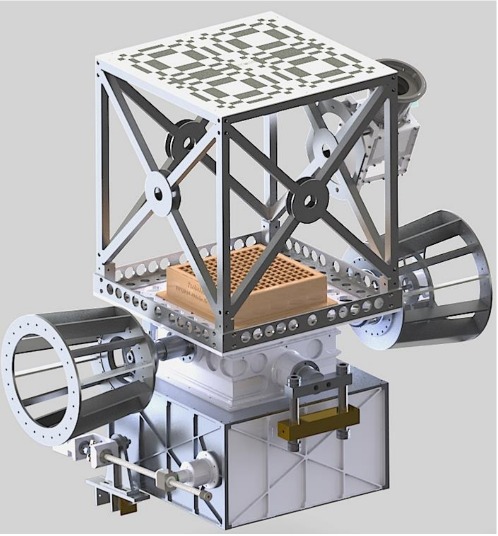

J. Braga et al., "**The protoMIRAX hard X-ray imaging balloon experiment**," Astron. & Astrophys., **Volume** 580, August 2015

Hexagonal Coded Aperture

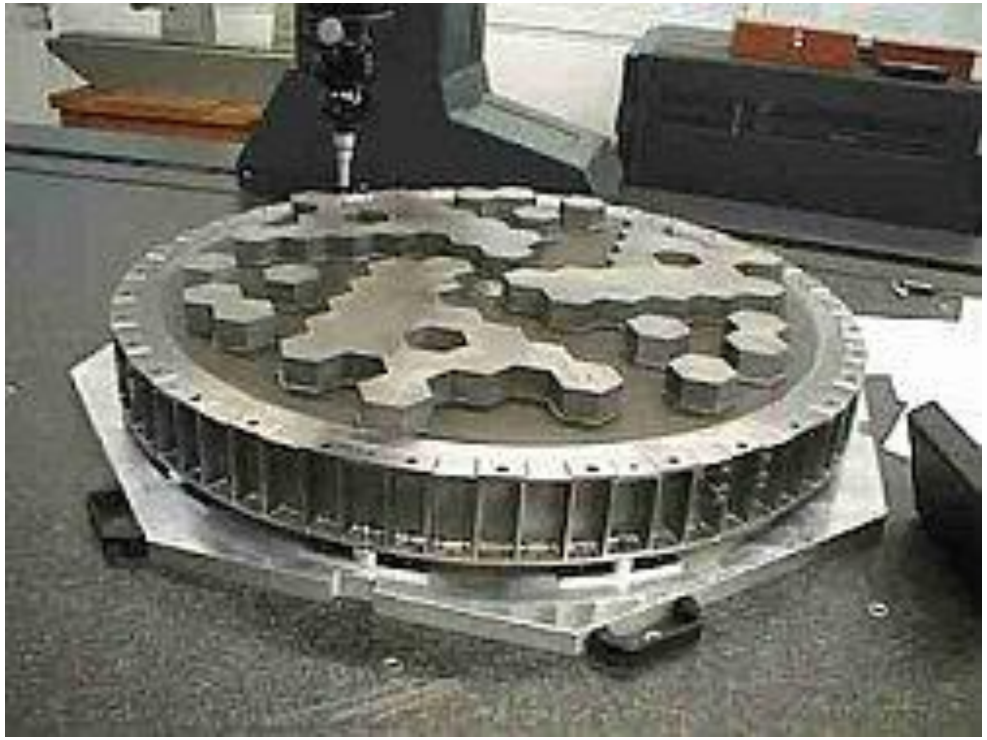

http://stratocat.com.ar/stratopedia/192.htm

Coded Aperture Image Reconstruction

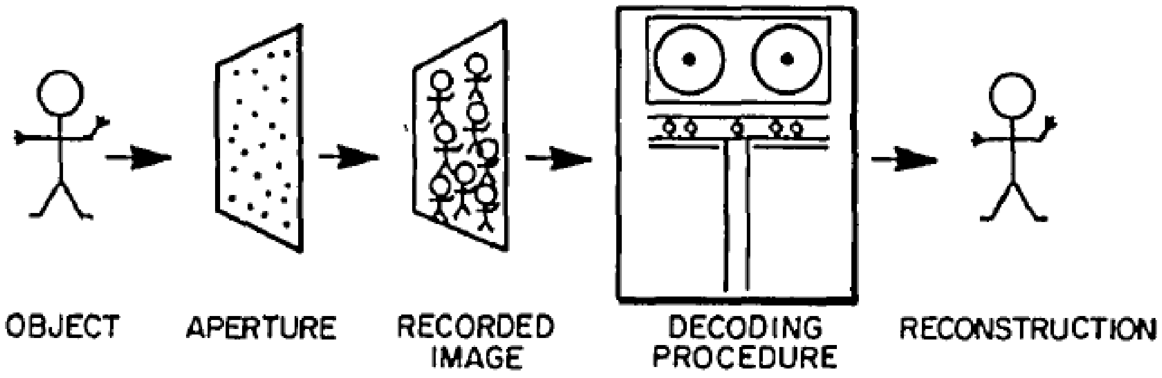

If the recorded picture is represented by the function P, the aperture by A and the object by O,

$$P = (O * A) + N, \quad (1)$$

where $*$ is the correlation operator and N is some noise function.

Fast reconstruction methods:

Fourier transform method: the object is solved for by

$$\hat{O} = R\mathcal{F}^{-1}[\mathcal{F}(P)/\mathcal{F}(A)] = O + R\mathcal{F}^{-1}[\mathcal{F}(N)/\mathcal{F}(A)], \quad (2)$$

where $\mathcal{F}$, $\mathcal{F}^{-1}$, and R are, respectively, the Fourier transform, the inverse Fourier transform, and the reflection operator.

Drawback:
→Sensitive to noise, depending on mask pattern

Correlation method: the reconstructed object is defined to be

$$\hat{O} = P * G = RO * (A * G) + N * G, \quad (3)$$

where G is called the postprocessing array and is chosen such that $A * G$ approximates a delta function.

Advantage:
→Less sensitive to noise than fourier method

E.E. Fenimore and T.M. Cannon, Appl. Optics, V17, No. 3, p. 337 (1978).

URA design principles

A   G   A*G

Modified URA Mask, Anti-mask, and Cross-correlation

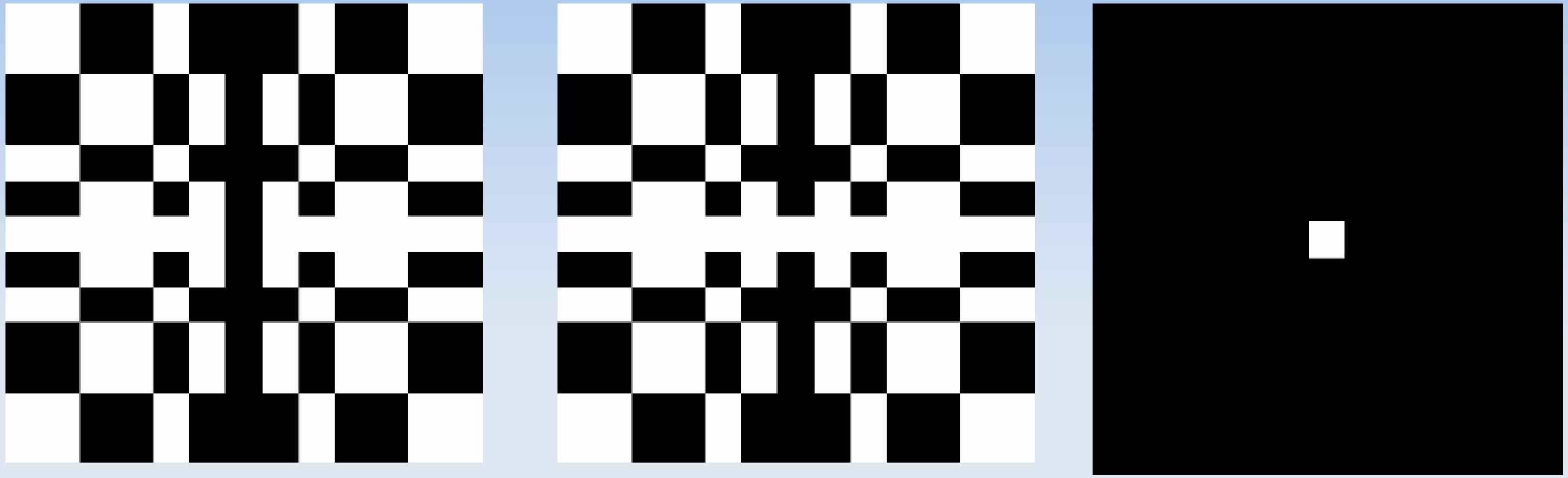

- Image is encoded using mask and decoded using anti-mask, where cross-correlation between mask and anti-mask is delta function.
- Pixel transparency determined by Jacobi function:
  - Is (pixel index)%DIM == (i*i)%DIM for any 1<i<DIM?
    - Yes/No->Open/Closed.
    - 2-D case based on inverse XOR of both indices.

E.E. Fenimore and T.M. Cannon, Appl. Optics, V17, No. 3, p. 337 (1978).

Key point:
Cyclic cross-correlation A*G is a perfect **delta function**

URA:

$$G(I,j) = \begin{cases} 1 & \text{if } A(I,j)=1 \\ -1 & \text{if } A(I,j)=0 \end{cases}$$

Modified URA (MURA):
Same as above, plus

$$G(I,j) = 1 \text{ if } i+j=0$$

Coded Aperture Image Reconstruction

- **In practice**, due to issues of dealing with background and detector noise, many practical applications of coded aperture imaging for x-ray astronomy have been based on iterative methods, rather than direct deconvolution.
  - Modify proposed source distribution until it generates similar image to measured detector image.
  - In astronomy, one does not know what the source distribution should look like, and it is important not to create spurious sources through reconstruction artifacts.
- For accelerator-based measurements, we have additional issues due to not operating in classical limit, which direct reconstruction method assumes:
  - Diffraction effects
  - Spectral response of detector, and variation of spectrum on- and off-axis of SR fan
  - Non-uniform intensity profile of incident beam, unlike what can be assumed for astronomical sources.
- For accelerator beam measurement, we have thus far made use of **template fitting**:
  - Create an array of simulated detector images for different beam sizes and position offsets, and fit measured detector image against these templates to find the closest match.
  - Very brute-force, but with multi-cpu reconstruction machines, we can keep up with measurement rates of 1 to a few Hz for ~1 million templates.
  - Works because we generally know what the source distribution should look like: usually a single gaussian of unknown size and position, to be determined.

Template construction: What the detector sees

•Source SR wavefront amplitudes:

$$\begin{bmatrix} A_\sigma \\ A_\pi \end{bmatrix} = \frac{\sqrt{3}}{2\pi}\gamma\frac{\omega}{\omega_c}\left(1+X^2\right)(-i)\begin{bmatrix} K_{2/3}(\eta) \\ \frac{iX}{\sqrt{1+X^2}}K_{1/3}(\eta) \end{bmatrix},$$

where

$$X = \gamma\psi,$$

$$\eta = \frac{1}{2}\frac{\omega}{\omega_c}\left(1+X^2\right)^{3/2},$$

K.J. Kim, AIP Conf. Proc. 184 (1989).

J.D. Jackson, "Classical Electrodynamics," (Second Edition),John Wiley & Sons, New York (1975).

•Kirchhoff integral over mask (+ detector response) → Detected pattern:

$$A_{\sigma,\pi}(Detector) = \frac{iA_{\sigma,\pi}(Source)}{\lambda} \times \int_{mask} \frac{t(y_m)}{r_1 r_2} e^{i\frac{2\pi}{\lambda}(r_1+r_2)} \left(\frac{\cos\theta_1 + \cos\theta_2}{2}\right) dy_m$$

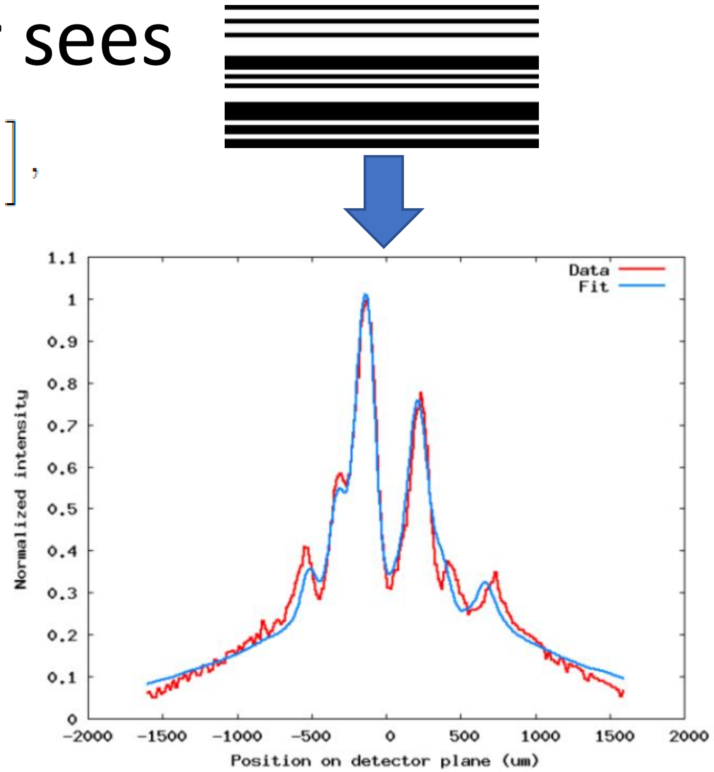

Measured slow-scan detector image (red) at CesrTA, used to validate simulation (blue)

- $t(y_m)$ is complex transmission of mask element at y_m.
- Sum intensities of each polarization and wavelength component.
- Sum weighted set of detector images from point sources.
  - The source beam is considered to be a vertical distribution of point sources.
  - Can also be applied to sources with non-zero angular dispersion and longitudinal extent, for more accurate simulation of emittance and source-depth effects.
  - For machines under consideration here these effects are small, so for computational speed we restrict ourselves to 1-D vertical distributions.

If template fitting, what are advantages of URA mask pattern?

- Advantage over simple pinhole/slit:
  - Greater open aperture for single-shot measurements
    - Particularly useful for low-current studies
      - At SuperKEKB, optics tuning is done at low currents to protect the detector from beam-loss backgrounds, before ramping back up to full currents for collision data-taking.
      - Optics group needs beam sizes at low currents to evaluate tuning effectiveness.
  - Somewhat better resolution
    - Get some peak-valley ratios that help at smaller beam sizes.
    - Make use of more of the detector, improve S/N
- What about a simple equal-spaced array of pinholes/slits?
  - Flatter spatial frequency response with URA
    - Better chance of matching shape without artifacts
    - Unique position determination (non-repeating pattern)
  - On the other hand, an equal-spaced array can offer tuned resolution over a narrower range of sizes
    - Equal-spaced array may be suitable for a very stable machine, such as a light source.
- For instability studies (e-cloud, e.g.) or other machine studies, or for a luminosity machine which is always running at the limit of stability, a URA mask promises better performance over a range of bunch conditions.

Other x-ray imaging approaches at accelerators: X-ray focusing optics

Fresnel Zone Plates (ATF)

- Open aperture: 50%

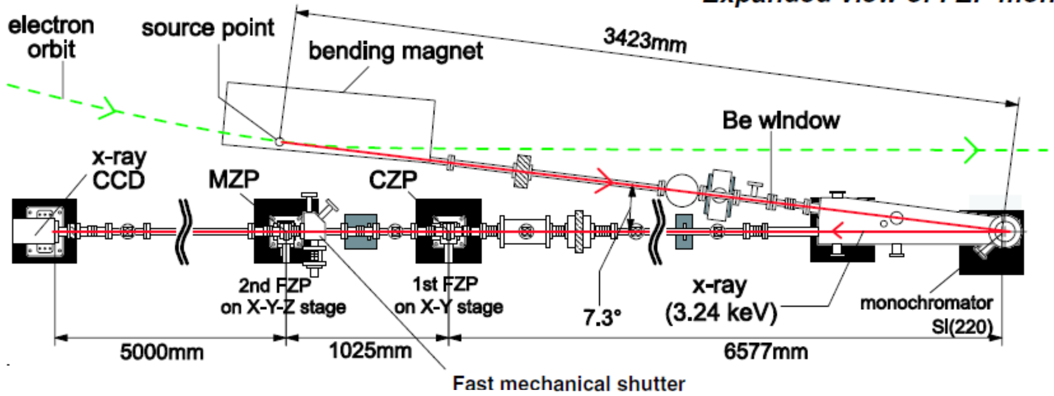

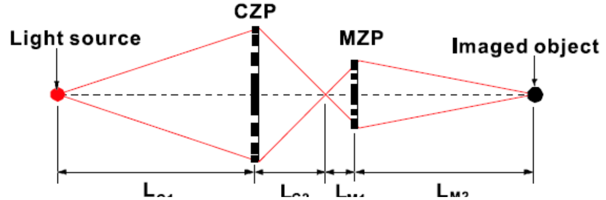

H. Sakai, et al., PRST-AB 10 042801 (2007).

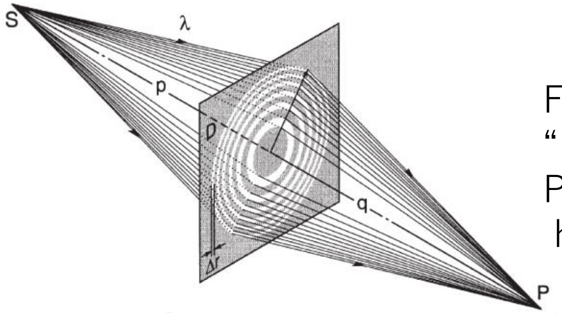

Figure from: A. Thompson et al., "Handbook of X-ray Optics," LBNL PUB-490 Rev. 3, p. 4-2 2009. http://xdb.lbl.gov/xdb-new.pdf

Al Refractive Lenses (ESRF)

- Effective open aperture: Determined by attenuation (thickness) of Al

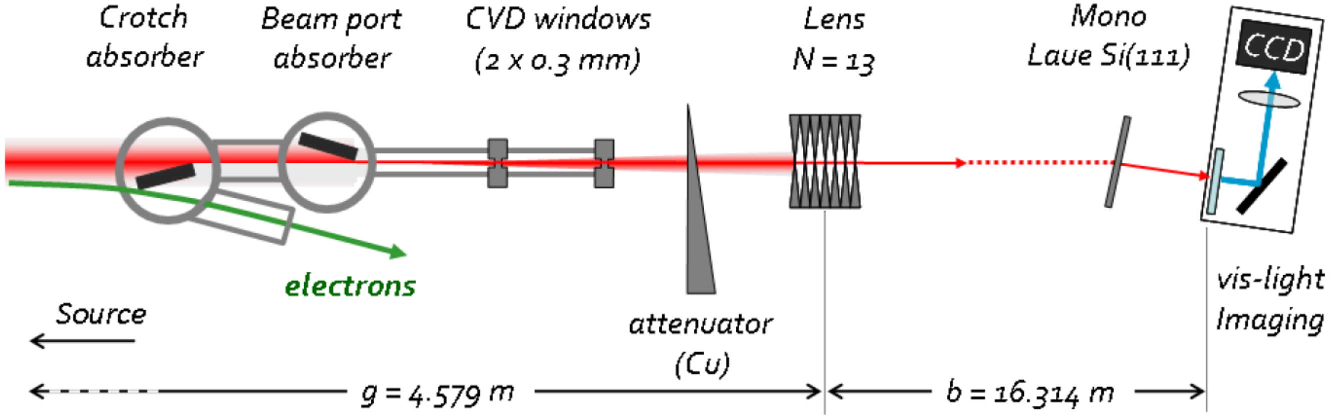

F. Ewald et al., "EMITTANCE MEASUREMENT USING X-RAY LENSES AT THE ESRF," Proc. IBIC2013, WEPF11, Oxford, UK, Sep. 2013

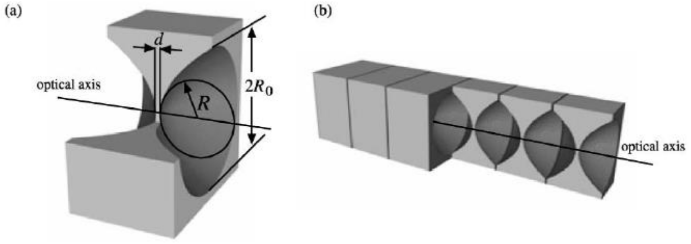

B. Lengeler *et al.*, "Parabolic refractive X-ray lenses: a breakthrough in X-ray optics ," NIM A 467-468 p. 944-950 (2001).

→Both options lose focusing resolution due to chromatic aberration as bandwidth increases

Introduction: Target machines

X-ray Source Parameters:

Parameter	**CesrTA (low-energy)**	**Diamond Light Source**	**ATF2** Extraction Line Bend BH3X	**SuperKEKB** Low Energy Ring / High Energy Ring
σ_y (μm) (minimum) (at x-ray source point)	~10	~7	a few	~10
Beam Energy (GeV)	2.085	3	1.3	4 / 7
Bending radius (m)	31.65	7.15	4.3	31.74 / 106
Critical Energy (keV)	0.64	8.4	1.12	4.5 / 7.2

Machines:

- CesrTA
  - ILC damping ring and low-emittance ring test machine, with focus on low-emittance tuning and electron-cloud studies.
- Diamond Light Source
  - Third generation light source.
- ATF2 (KEK)
  - ATF (ILC DR test machine) extraction line. ILC final focus optics and beam instrumentation test line.
- SuperKEKB
  - Super B factory: e+ e- two-ring energy-asymmetric collider for new physics searches.

Experience at Diamond LS

Beamline, detector:

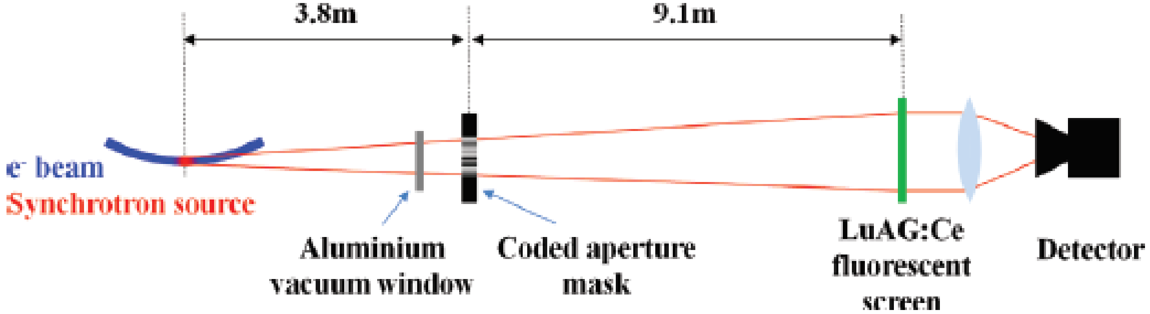

Figure 3: Basic schematic layout of the coded aperture beamline.

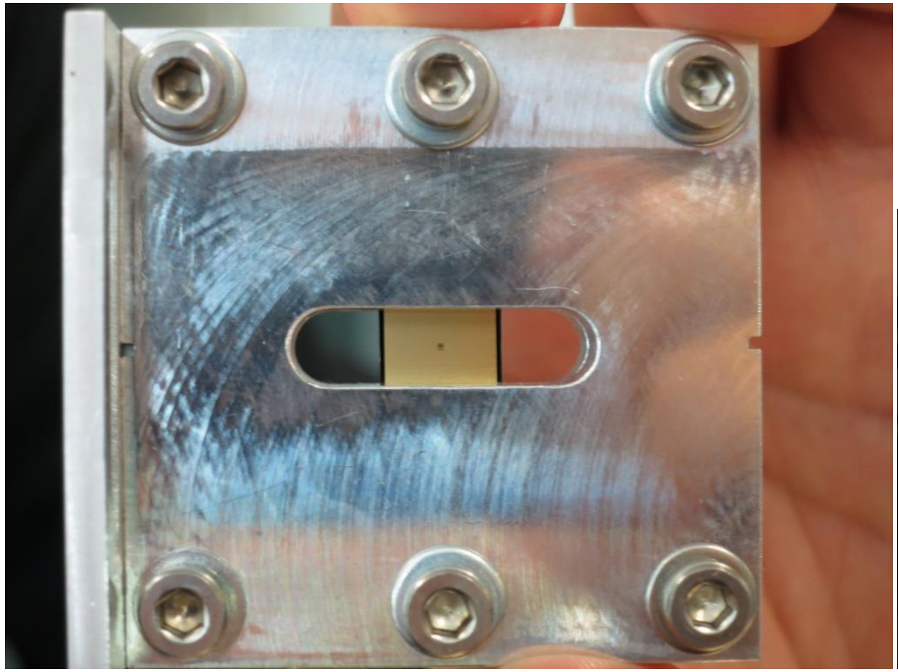

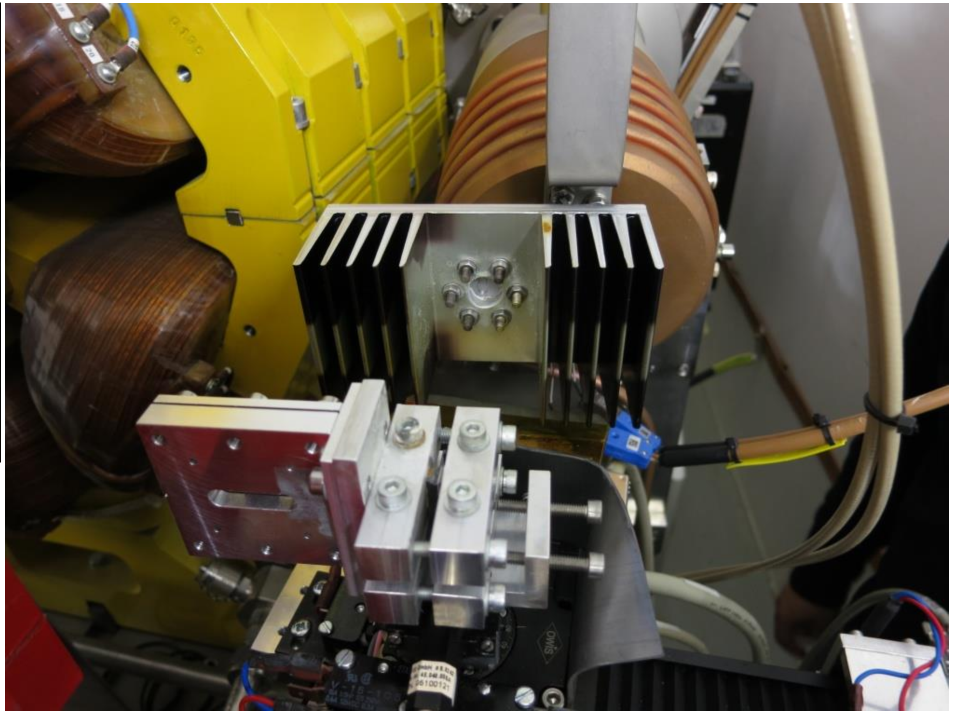

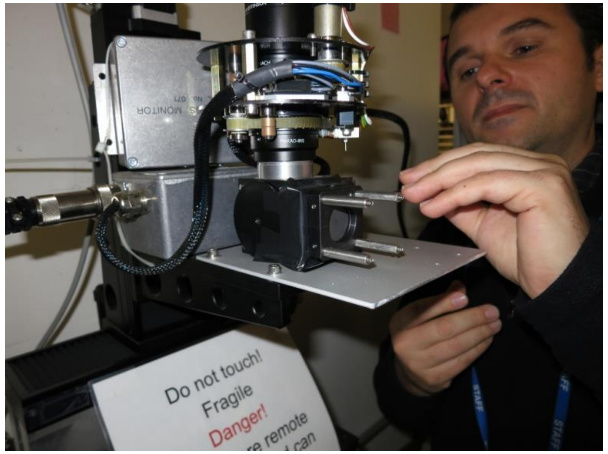

Experience at Diamond LS

Measurement results:

- Using spare high-energy optic (Au+Si) designed for SuperKEKB:
  - 10 μm x 59 URA
  - 18.2 μm Au mask on 625 μm Si substrate
- Detector:
  - 200 μm LuAG:Ce screen
  - 1024(H)x768(V) pixel camera
- **Not single-shot measurements, but sufficiently detailed data to demonstrate validity of fitting model.**

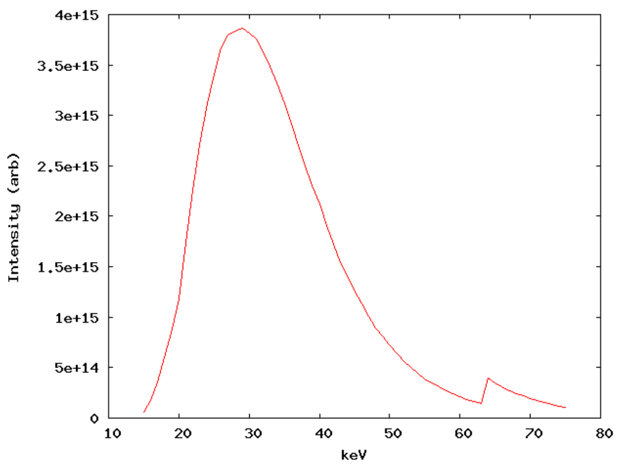

Modeled detected spectrum

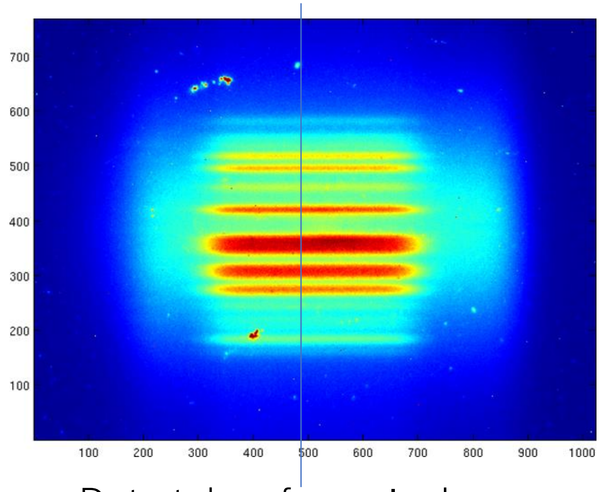

Data taken from single-pixel-width line near center

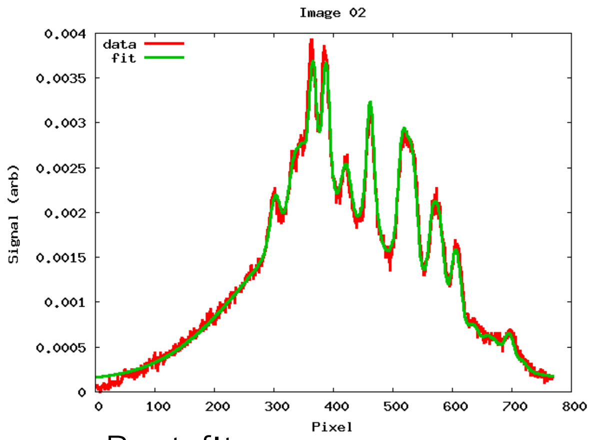

Best-fit:
--Beam size: 10.5 μm
--Mask position relative to beam: 166 μm

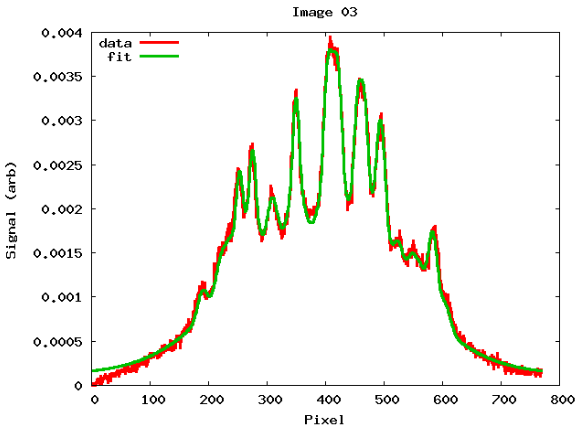

Best-fit:
--Beam size: 10.4 μm
--Mask position relative to beam: 5 μm

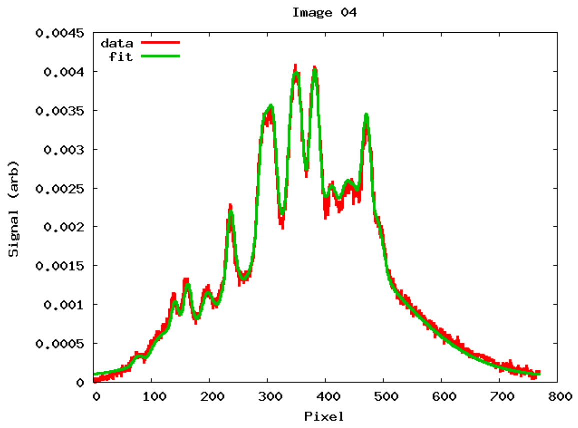

Best-fit:
--Beam size: 10.6 μm
--Mask position relative to beam: -126 μm

Experience at Diamond LS

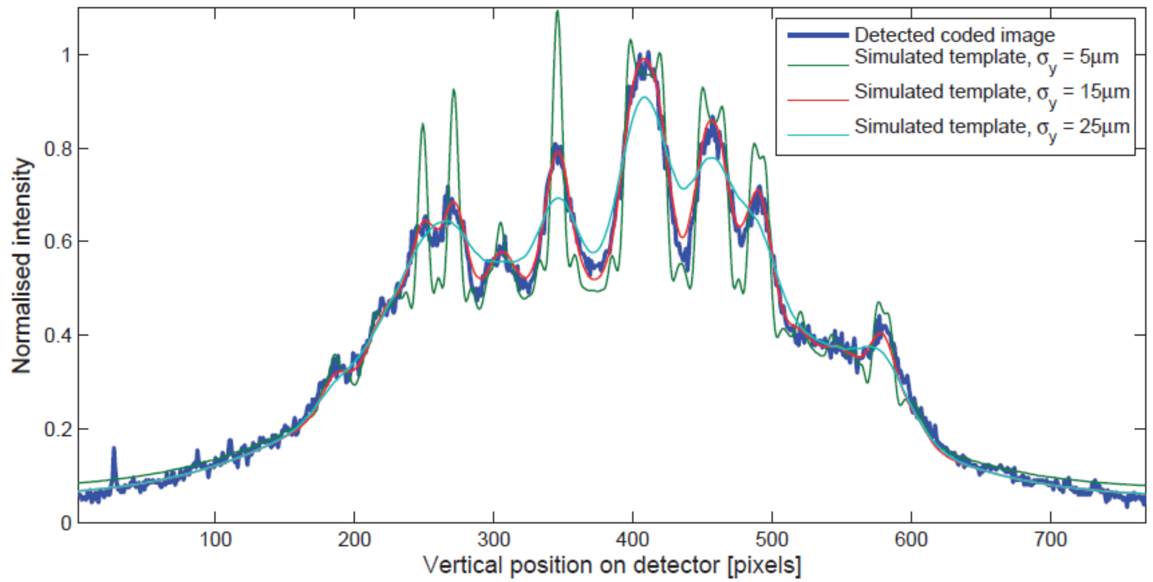

Figure 6: The detected flux for nominal beam conditions (~0.3 % coupling, κ) as seen by a single column of pixels from the camera, plotted along with the generated templates for flux seen at each detector pixel for three different vertical source sizes, σ_y.

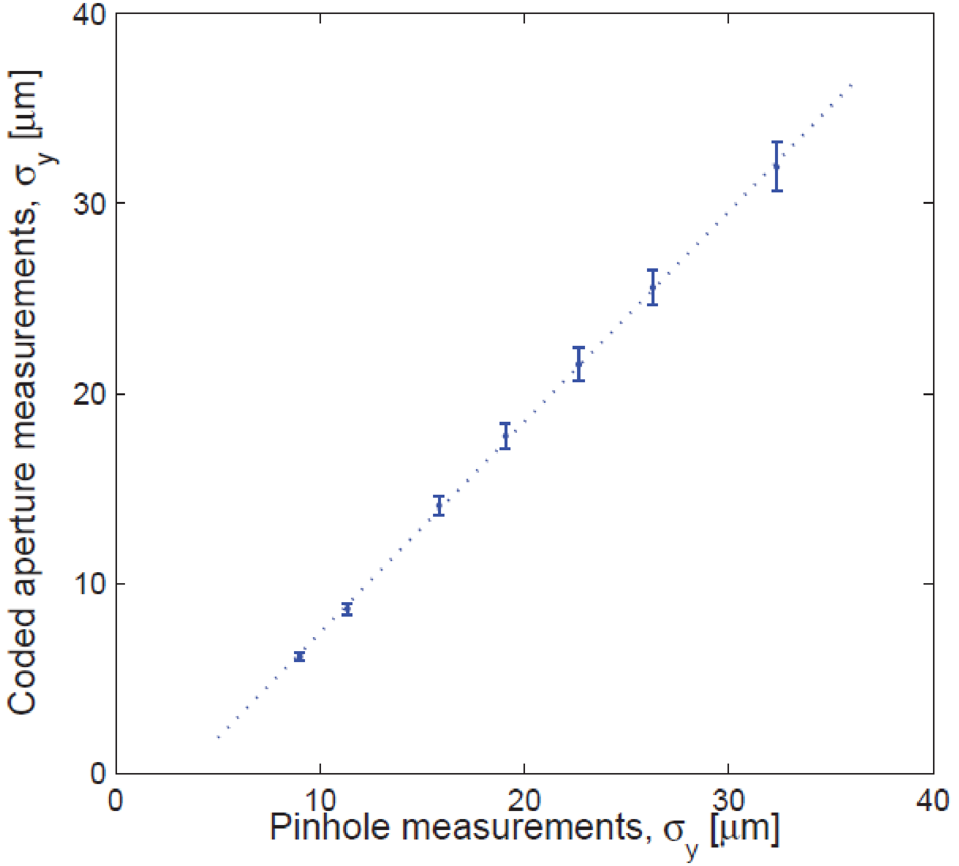

Figure 7: A plot comparing the vertical electron beam size measurements calculated from pinhole images, and calculated from from coded aperture images. A best fit line is shown.

The coded aperture measurements of vertical electron beam size correlate well with those measured by the existing pinhole cameras at DLS, although unexplained differences in the measured beam size are observed. The coded aperture measurements consistently give a smaller beam size than that found using the pinhole camera. Resolution of the coded aperture system is found to be on par with that obtained with the pinhole cameras, although the clear discrepancies between the measurements of the two systems require further investigation.

C. Bloomer, G. Rehm, J.W. Flanagan, "MEASUREMENTS OF SMALL VERTICAL BEAMSIZE USING A CODED APERTURE AT DIAMOND LIGHT SOURCE," Proceedings of IBIC2014, Monterey, CA, USA, p. 279 (2014)

Experience at CesrTA

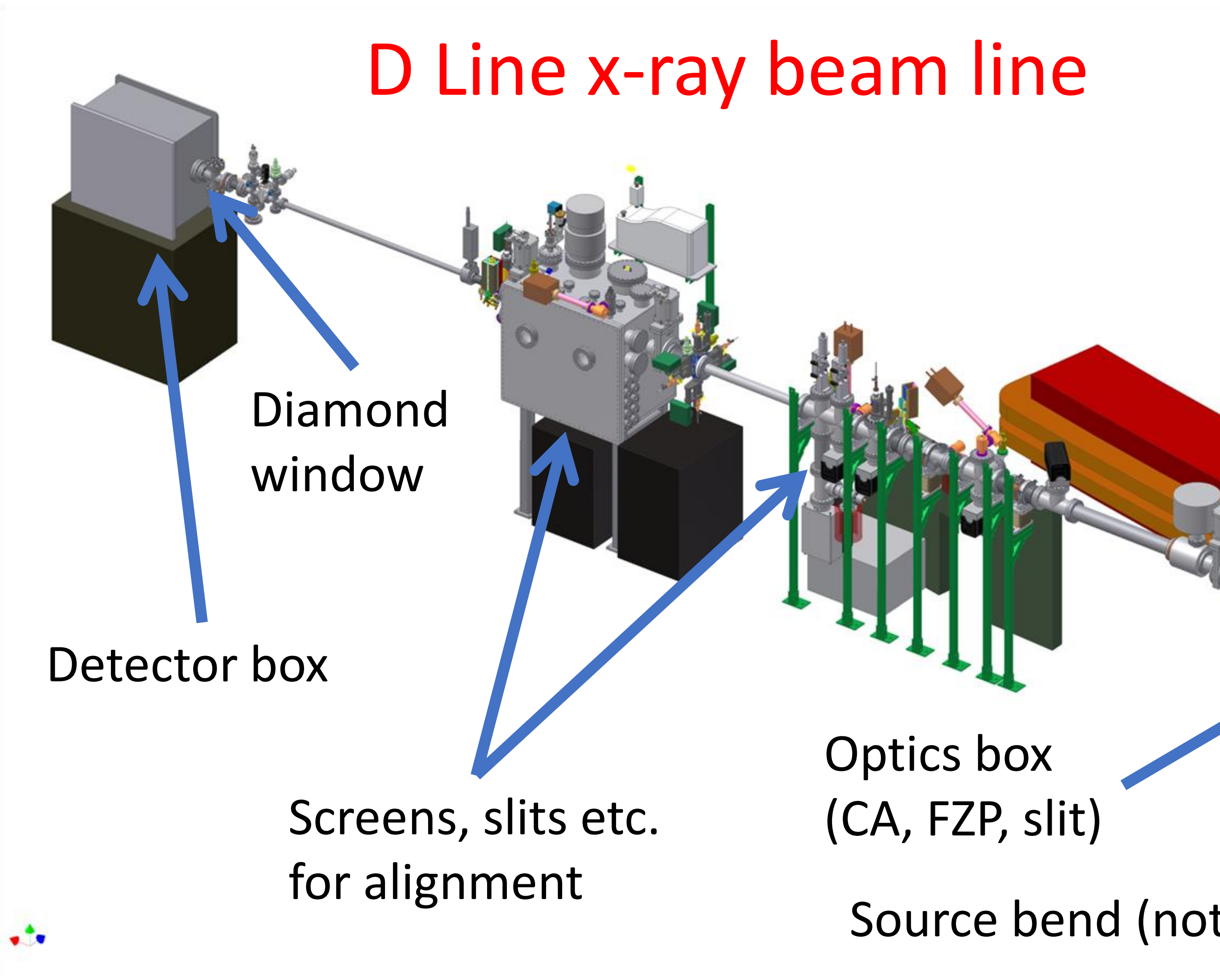

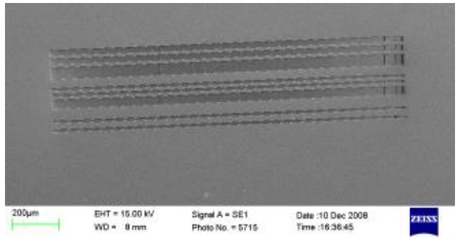

CA mask
(Applied Nanotools)
0.5 μm Au mask
2.5 μ Si substrate

CesrTA: Data Analysis

- 1) Simulate point response functions (PRFs) from various source positions to detector, taking into account beam spectrum, attenuations and phase shifts of mask and beamline materials, and detector response.
- 2) Add PRFs, weighted to possible proposed beam distributions.
- 3) Find best fit to detector data.

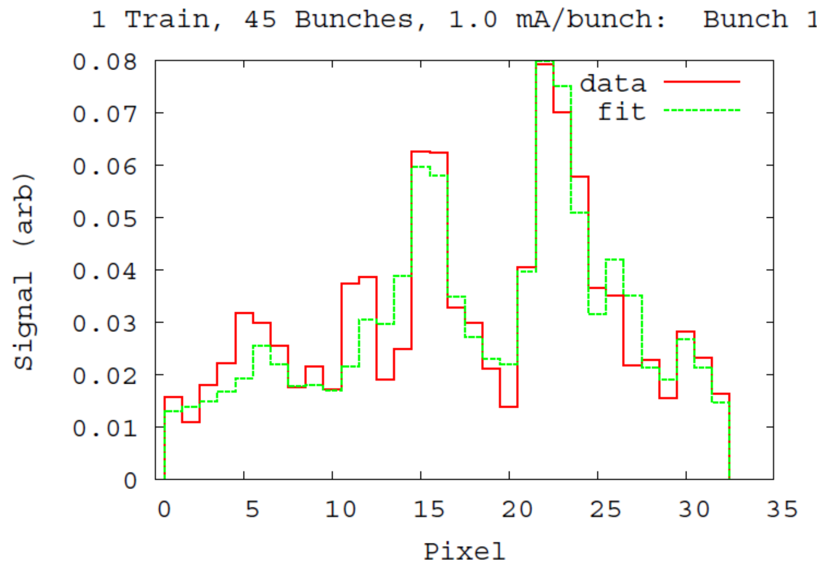

Example of single-shot data (single-bunch, single-turn)

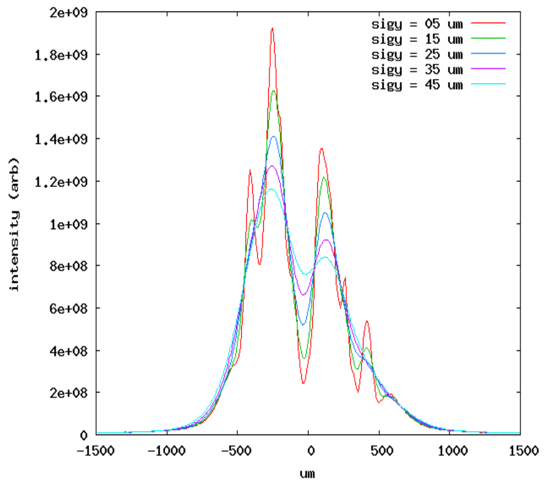

Simulated detector image for various beam sizes at CesrTA

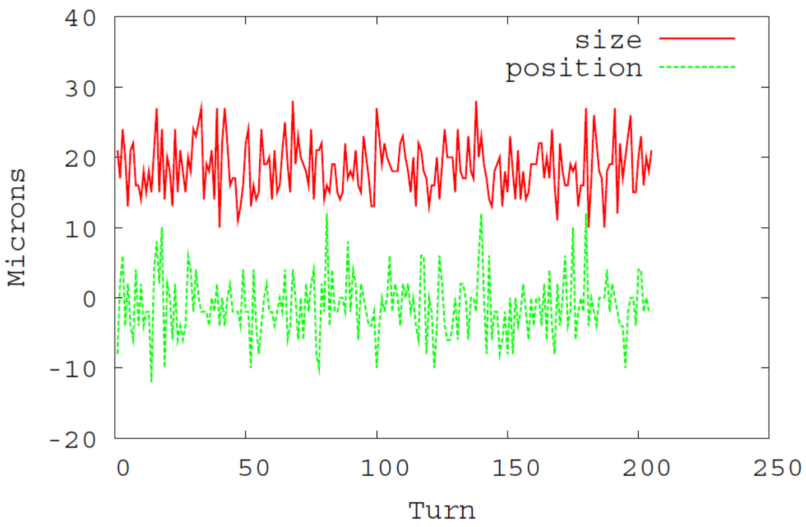

Example of turn-by-turn data (one bunch out of train)

CesrTA: Electron-cloud study data

- Study of effect of electron clouds on beam size.
- As cloud density increases along train, size of bunch increases due to presence of clouds.
- We can use this range of sizes to compare with resolution estimates.
    - Compare spread of sizes at each bunch with calculated resolution confidence intervals.

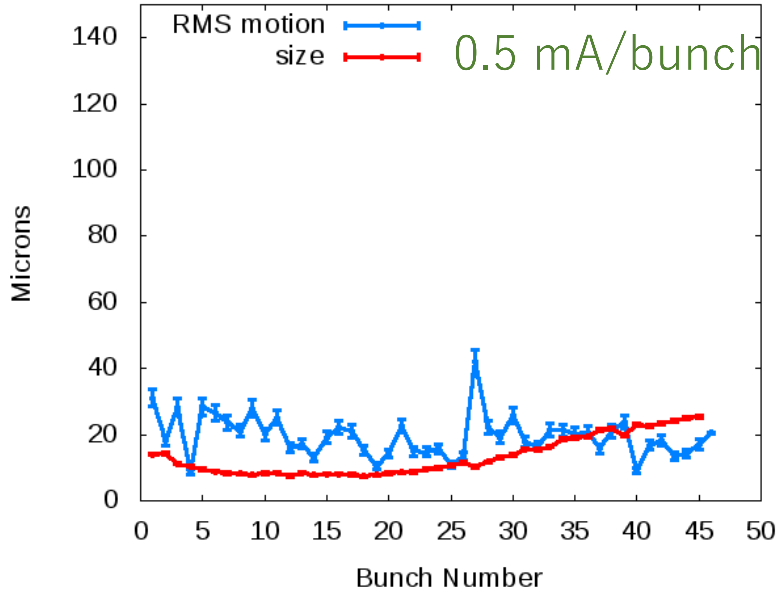

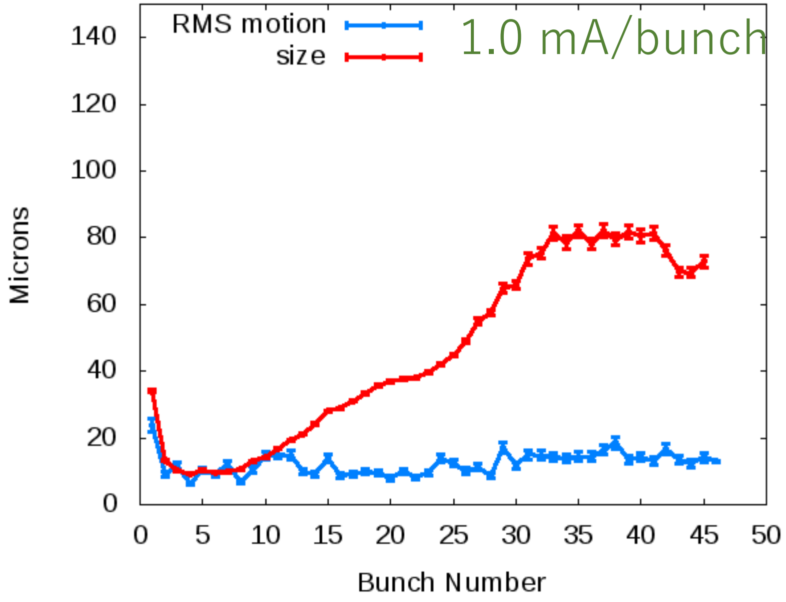

Single-shot resolution estimation

- Want to know, what is chance that a beam of a certain size is misfit as one of a different size?
- Tend to be photon statistics limited. (Thus coded aperture.)
- So:
  - Calculate simulated detector images for beams of different sizes
  - "Fit" images pairwise against each other:
    - One image represents true beam size, one the measured beam size
    - Calculate χ^2/ν residuals differences between images:

N = # pixels/channels
n = # fit parameters (=1, normalization)
S_i = expected number of photons in channel i

$$\frac{\chi^2}{\upsilon} = \frac{1}{N-n-1}\sum_{i=1}^{N}\frac{[s_i' - s_i]^2}{\sigma_i^2},$$

    - Weighting function for channel i:

$$\sigma_i = \sqrt{s_i}.$$

  - Value of χ^2/ν that corresponds to a confidence interval of 68% is chosen to represent the 1-s confidence interval

10 μm, 31-element CA mask @ D Line 2 GeV

Generate detector images for various beam sizes:

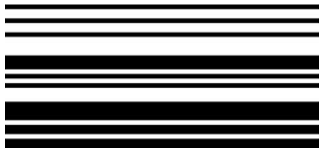

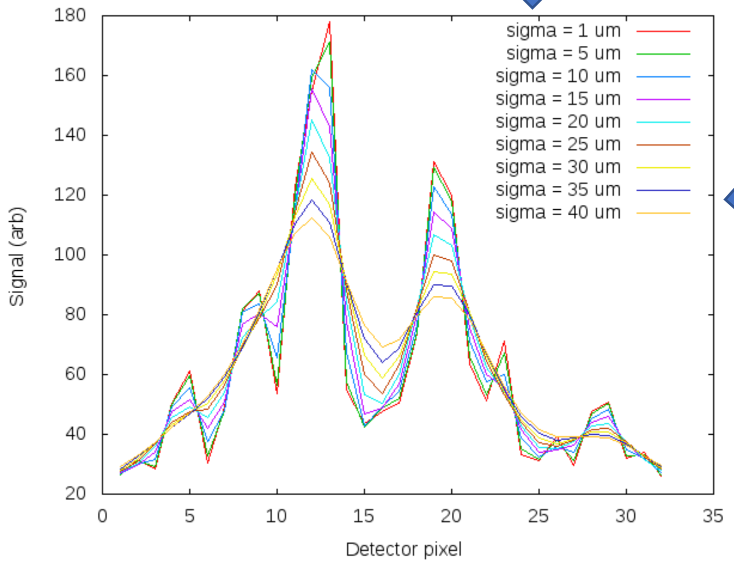

Cross-fit between beam sizes.
Plot 1-sigma statistical confidence regions,
Assuming 200 photons/pixel average
(=> 0.56 mA at 2 GeV):

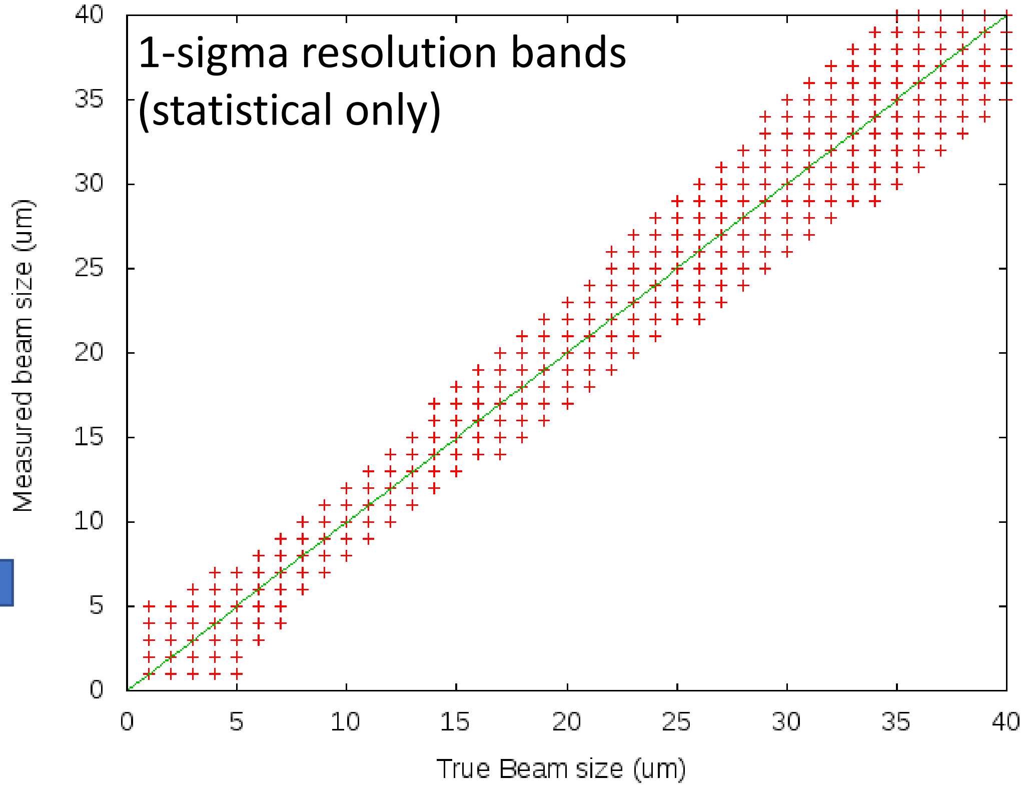

Statistical single-shot resolution at 10 μm beam size = +/- ~2 μm
(Assuming ideal detector.)

CesrTA: Resolution data vs simulation with CA

- Using May 10 2010 E-Cloud study data as data source.
- Simulation statistical confidence bands assume
  - Perfect, noiseless detector
  - 200 photons/pixel/shot on average
    - =>0.56 mA/bunch
- Shot-by-shot spread in data is between that at 0.5 mA and 1.0 mA in the data
  - Not using a perfect, noiseless detector.

- Reasonable agreement

- For more detailed evaluation, including effects of detector noise, see below:

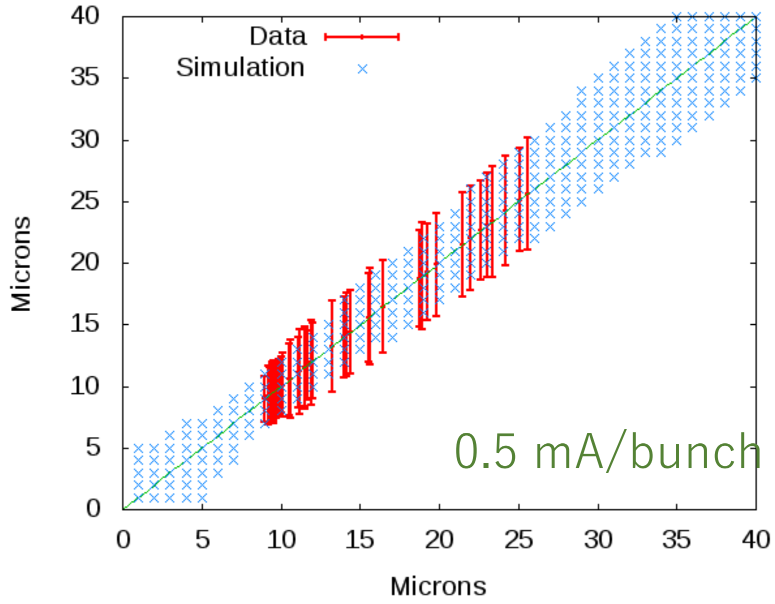

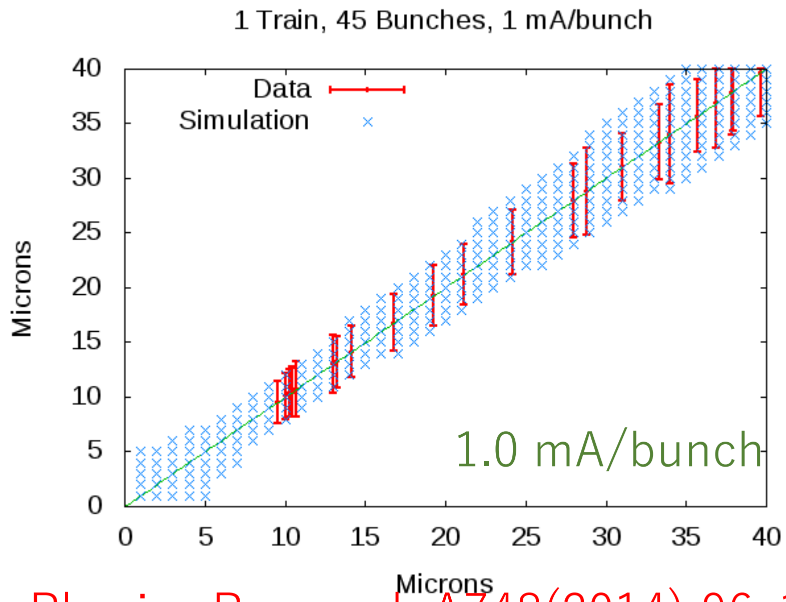

J.P. Alexander et al., Nuclear Instrumentsand Methods in Physics Research A748(2014) 96–125

CesrTA Alternate CA: Make use of interference peaks

URA

Enhanced diffraction peak design (Dan Peterson)

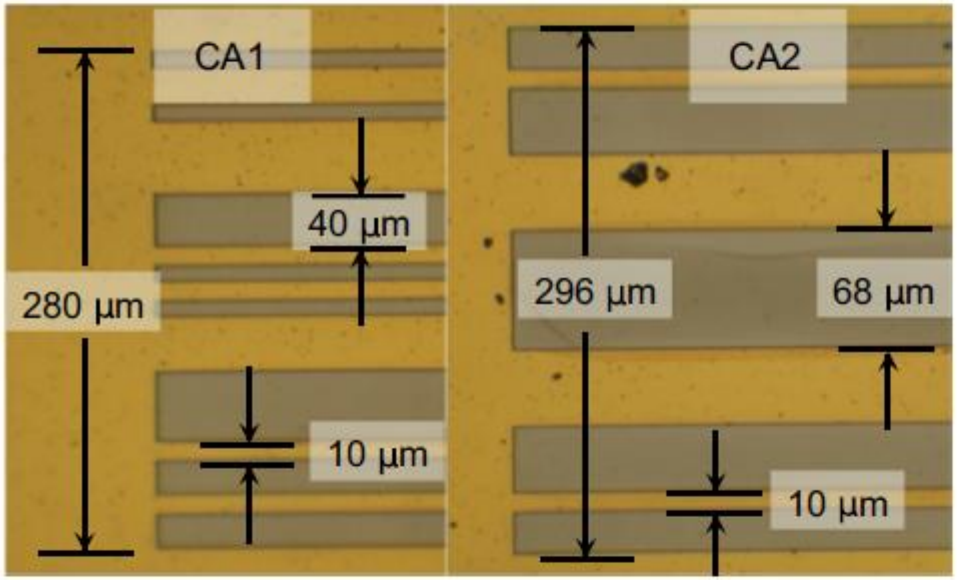

Fig. 2. Photographs of portions of CESR-TA xBSM coded aperture optical elements CA1 (left) and CA2 (right). Dark strips indicate transmission slits, while lighter areas represent the gold coating. The imperfections (black spots) are remnants of etching resist with thickness ~0.01 μm, which are essentially transparent to x-rays.

CA2 design philosophy: intentionally optimize slit widths to enhance diffraction peaks over detectable spectrum to create sharper edges in PSF.

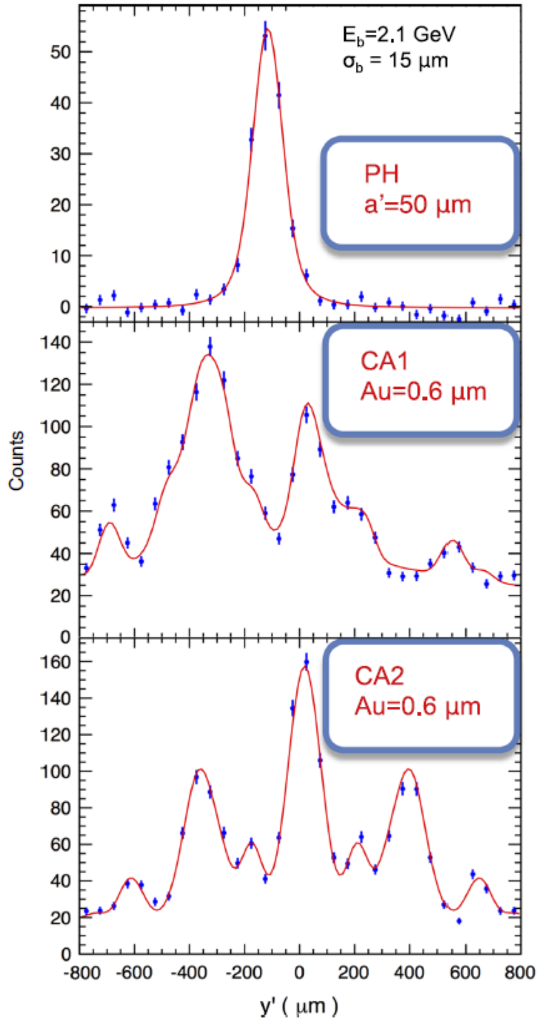

Fig. 4. Detector images (points with error bars) taken at $E_b = 2.1$ GeV using the PH (top), CA1 (middle), and CA2 (bottom) optical elements. The smooth curves show the best fits, which in all cases have $\sigma_b \approx 15$ μm.

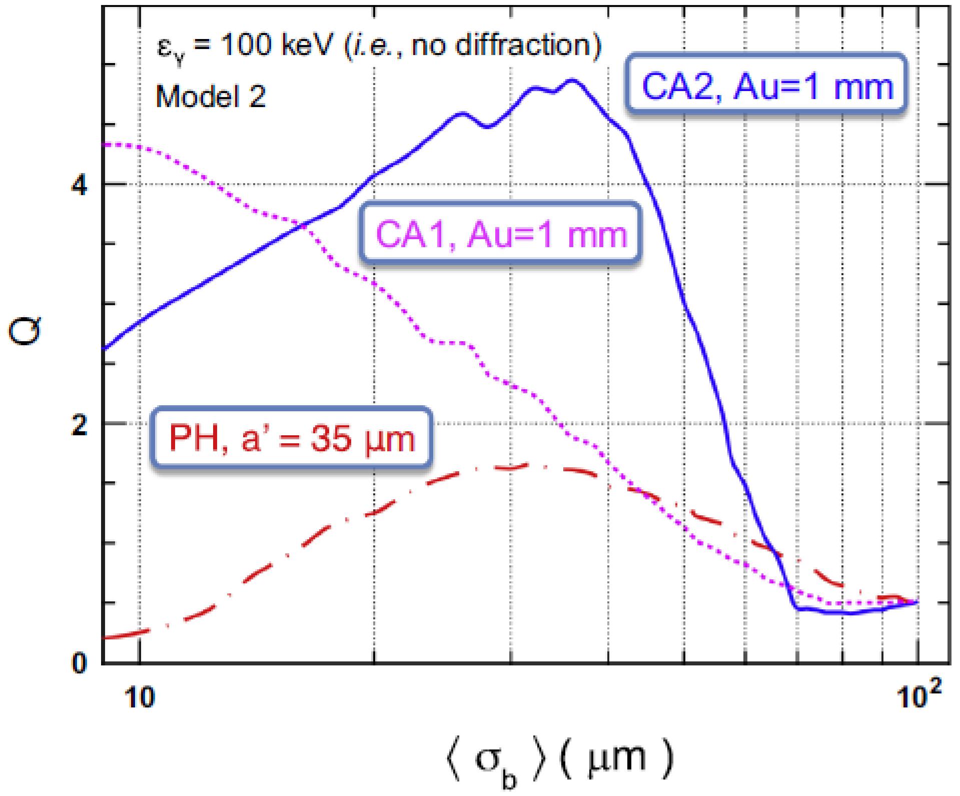

Fig. 12. Predicted figure of merit for each of three optical elements at CESR-TA in the non-diffractive, thick-masking limit.

J.P. Alexander et al., Nuclear Instruments and Methods in Physics Research A767(2014) 467–474

Coded Aperture tests at ATF2

During construction

Beam pipe from source bend with 200 μm Be window

Coded Aperture Mask

Beam pipe with Kapton windows

Detector

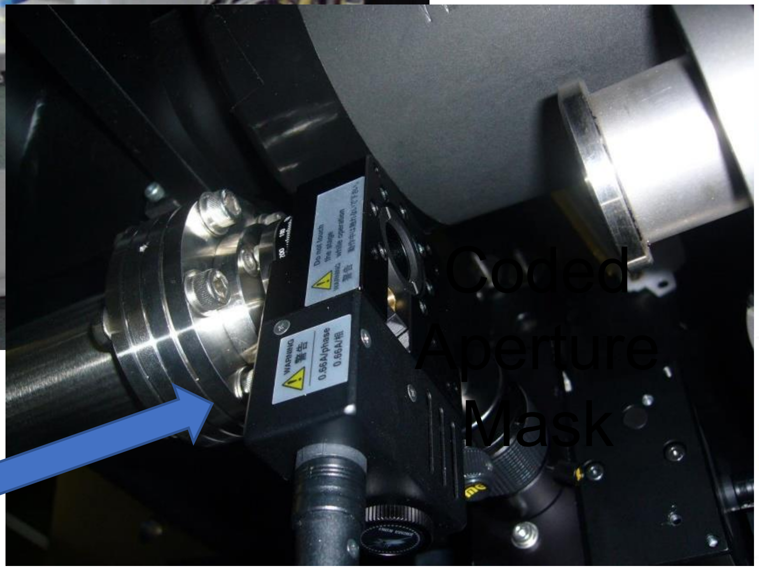

Rotating mask holder

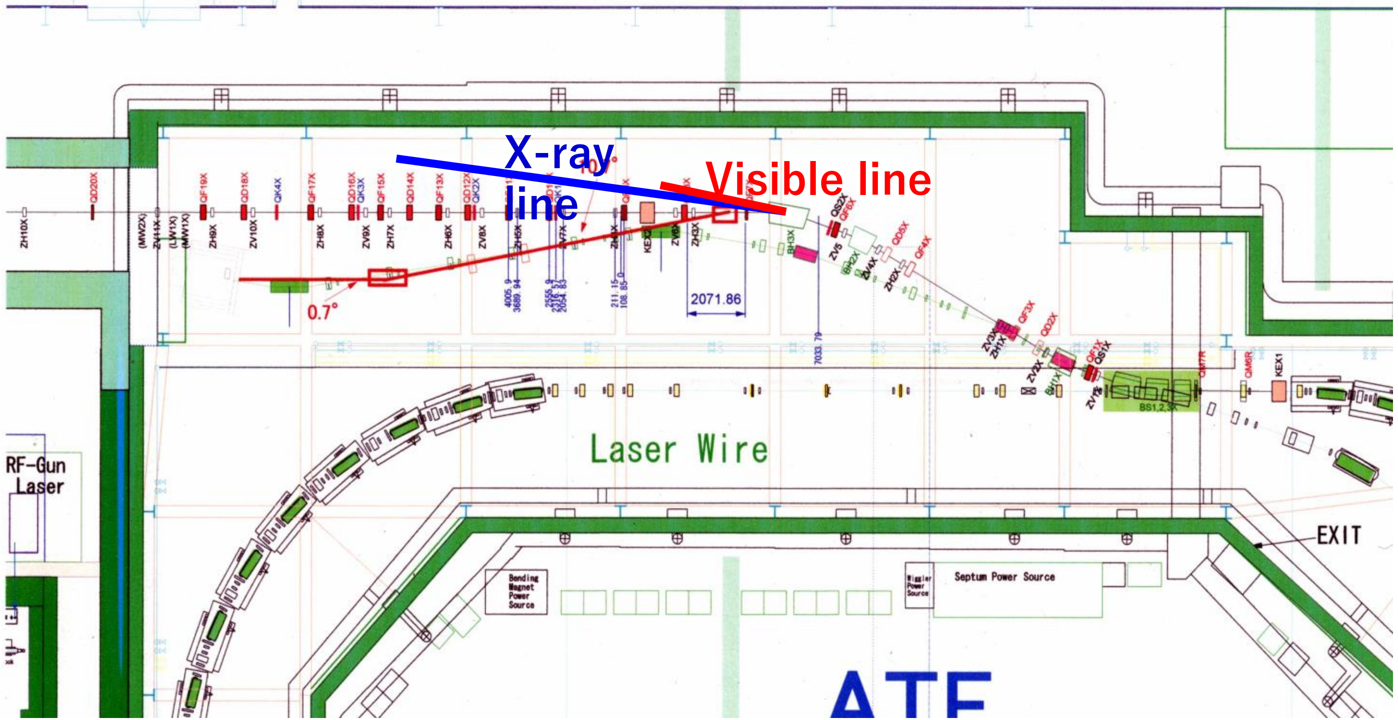

Coded Aperture tests at ATF2

Data taken by scanning single InGaAs pixel across detector plane

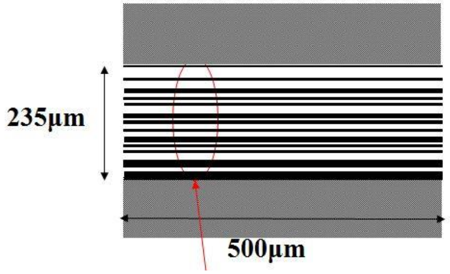

Data: Dispersion Knob Scans

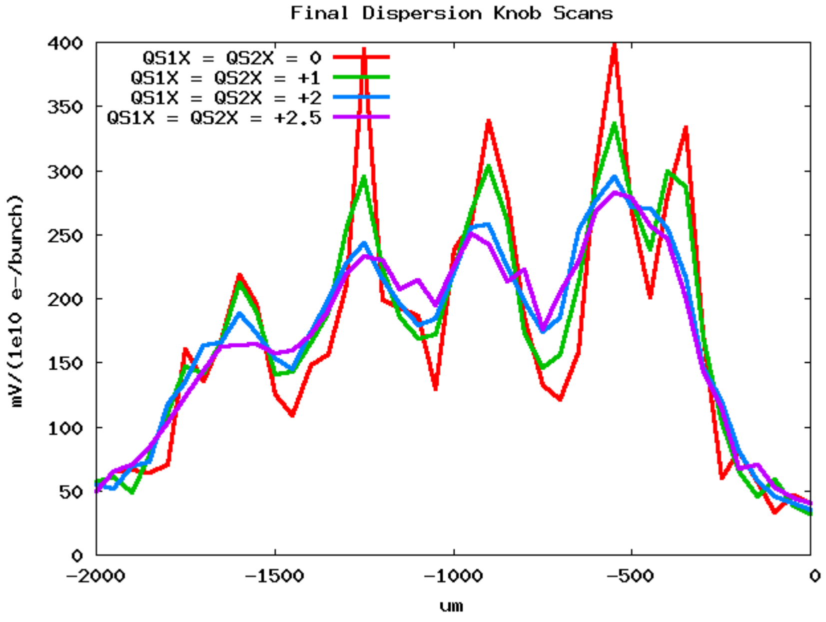

Simulations

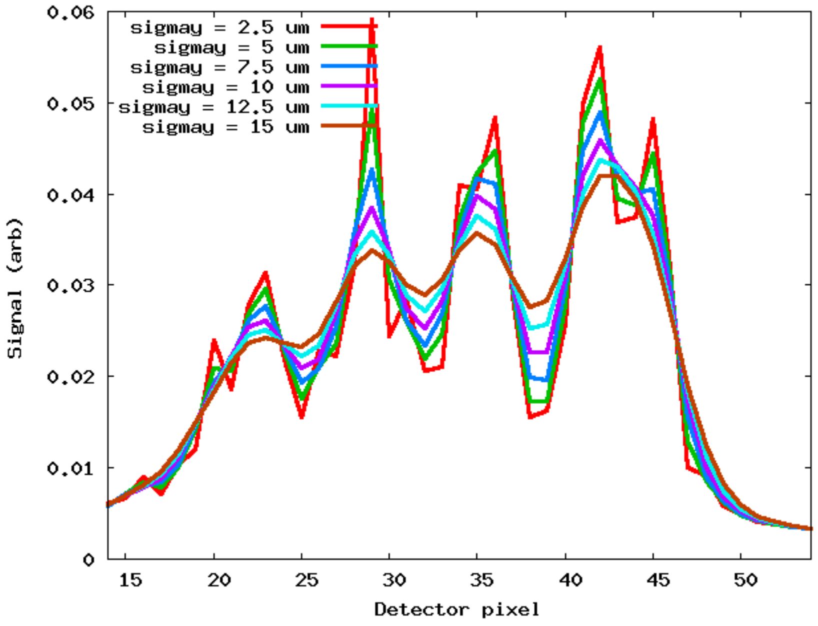

Measured beams of ~10 um with scanned-pixel measurements

SuperKEKB X-ray monitor

SuperKEKB is a 2-ring collider.
X-ray beam lines installed in both Low Energy Ring (LER) and High Energy Ring (HER).

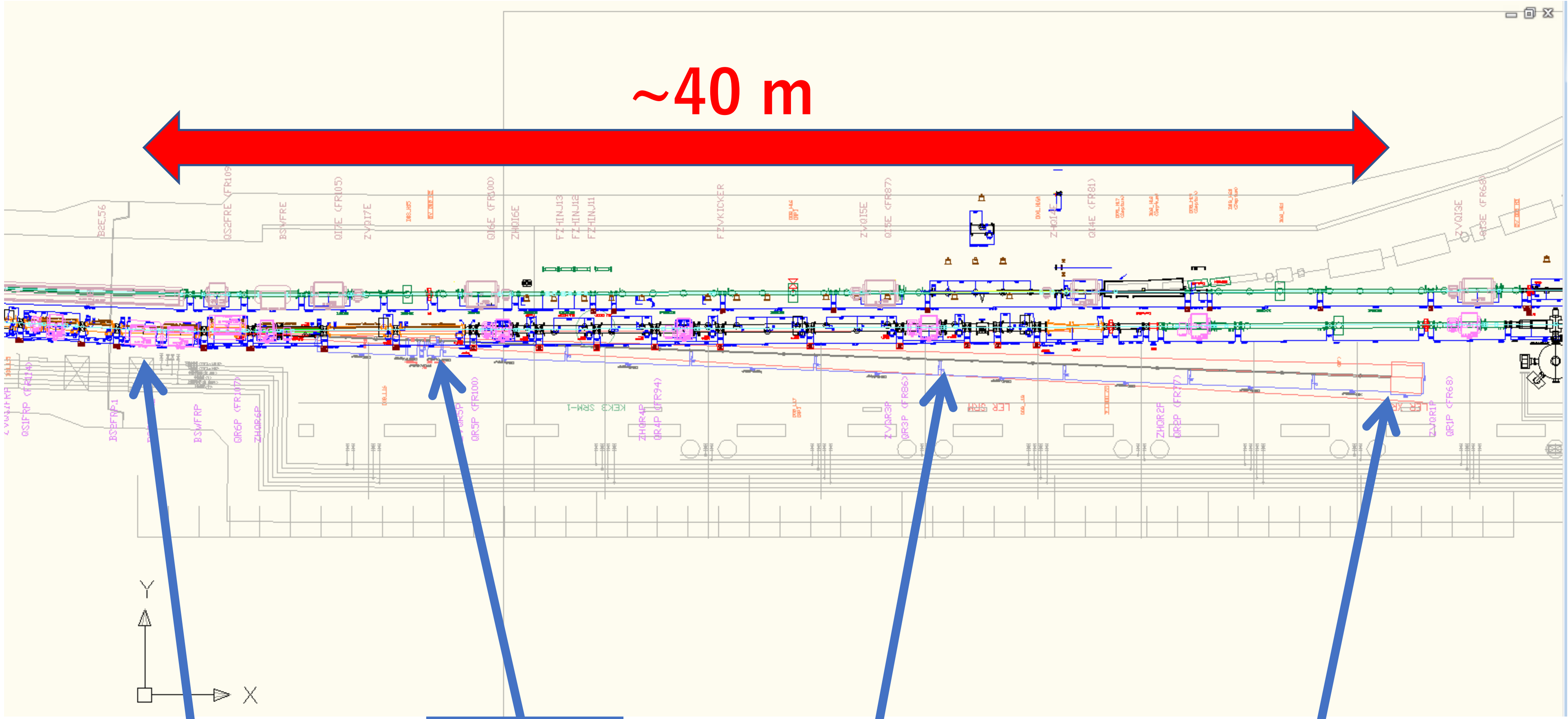

X-ray beam line at LER

Similar line also at HER

Source bend

Be filter, Optics box

X-ray beamline

Be Window, Detector

SuperKEKB X-ray beam profile Monitor

Mask patterns

Note: All three mask patterns based on units of optimal slit width for minimizing PSF.

Single slit: 33 μm

Multi-slit: 33 μm slits at varying spacings

URA: Slits and spacings are all multiples of 33 μm

Single slit, 33 μm wide

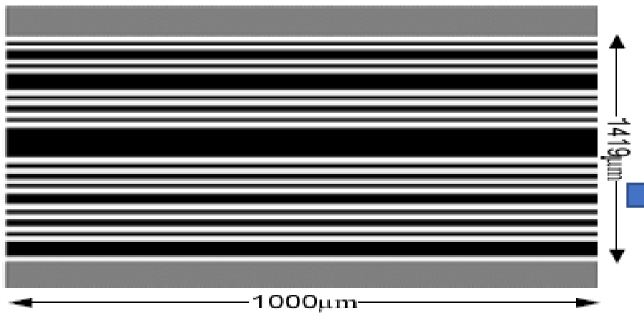

Multi-slit mask (E. Mulyani)

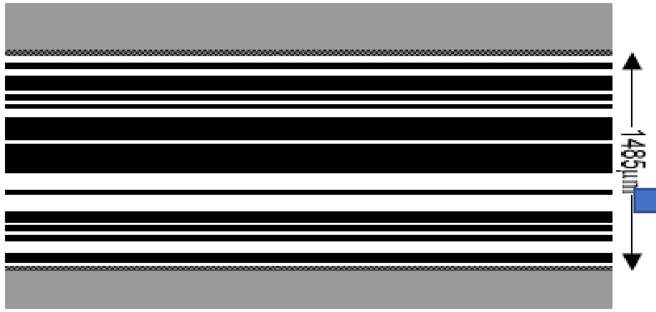

URA mask (E. E. Fenimore, T. M. Cannon, Appl. Optics, Vol 17, No.3, 337 (1978).

Calculated images for different beam sizes

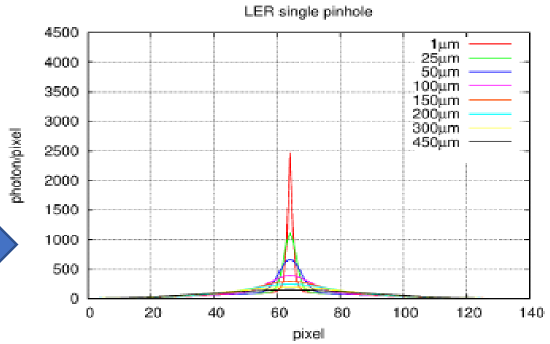

(a)

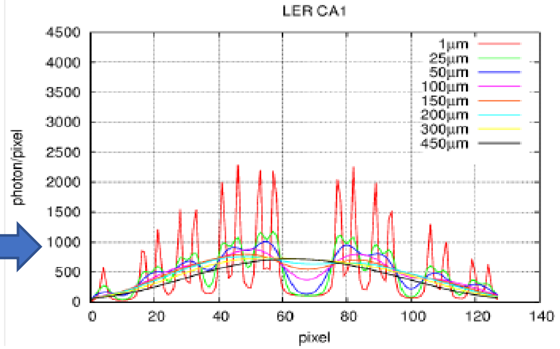

(b)

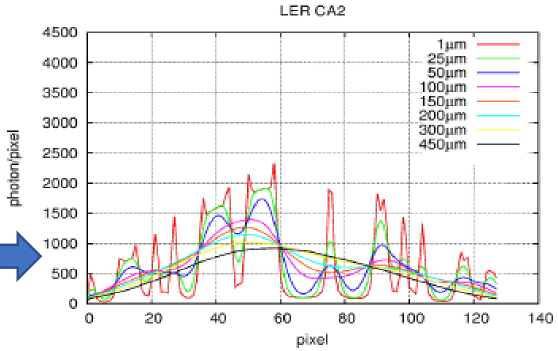

(c)

Figure 6: Simulated detector images showing the number of photons/pixel for 1 mA bunches for different beam sizes at LER: (a) single pinhole; (b) CA1; (c) CA2.

Single-shot statistical resolutions expected

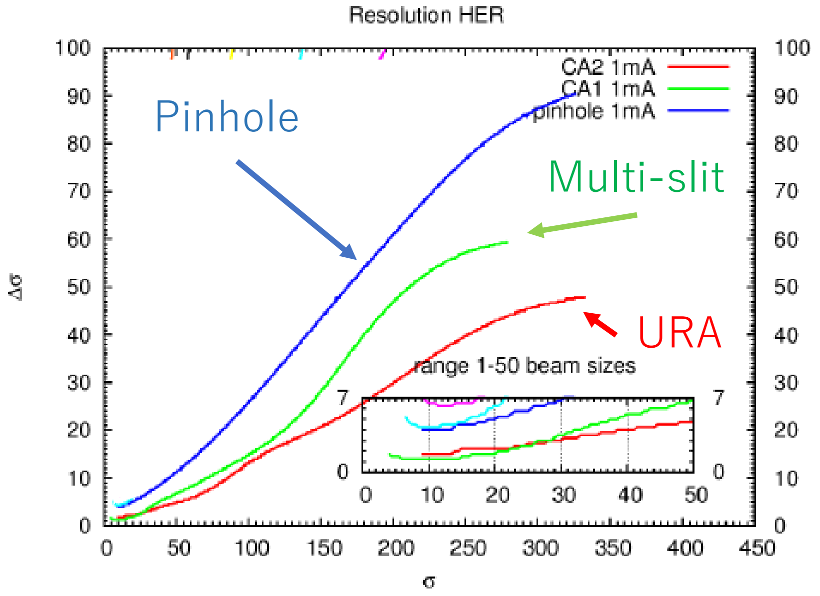

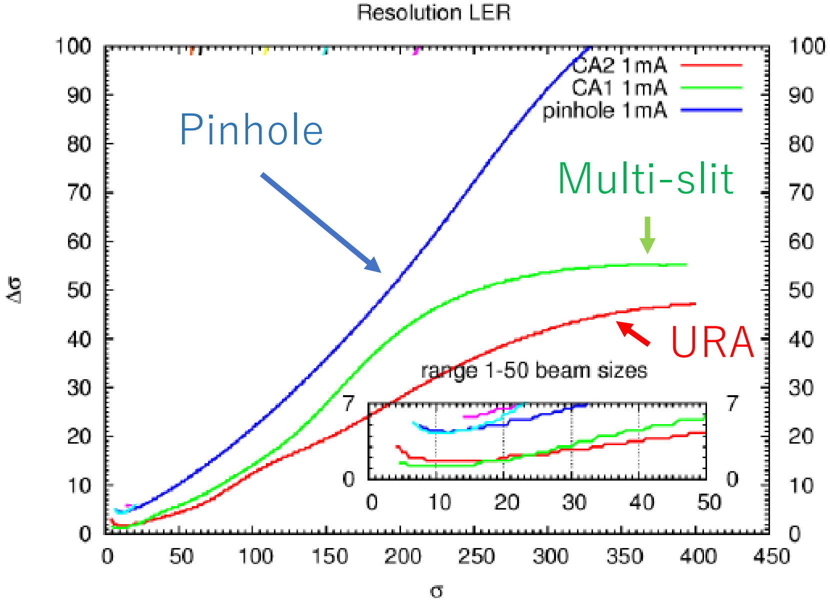

E. Mulyani and J. Flanagan, TUPB025, Proc. IBIC2015, Melbourne

SuperKEKB X-ray Monitor: Hardware

X–ray beam line under construction at LER

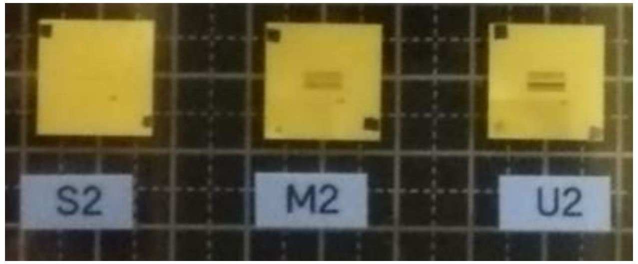

Masks: ~20 μm Au on 600 μm CVD diamond substrate

Water-cooled mask holder

US–Japan Collaboration (U. Hawaii, SLAC, Cornell U.)

High–speed readout electronics for the X–ray monitor, being developed by U of Hawaii.

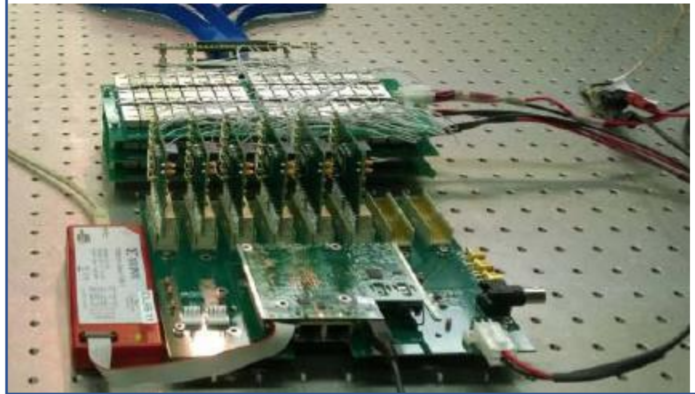

Deep Si pixel detector and spectrometer chips for the X–ray monitor, being developed at SLAC.

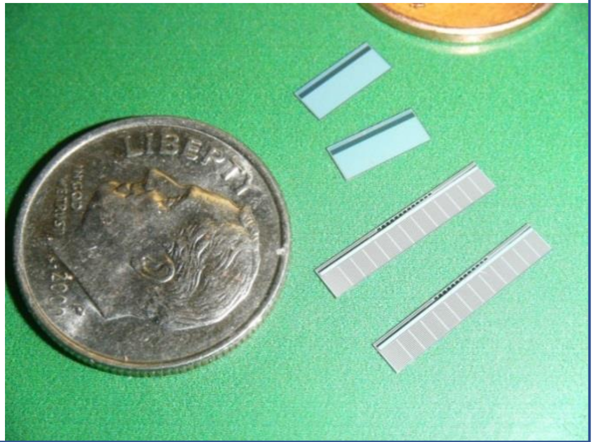

Scintillator read-out system for Phase I of SuperKEKB commissioning (Spring 2016)

E. Mulyani and J.W. Flanagan, "**CALIBRATION OF X-RAY MONITOR DURING THE PHASE I OF SuperKEKB COMMISSIONING**" Proceedings of IBIC2016, Barcelona, Spain (2016) 524.

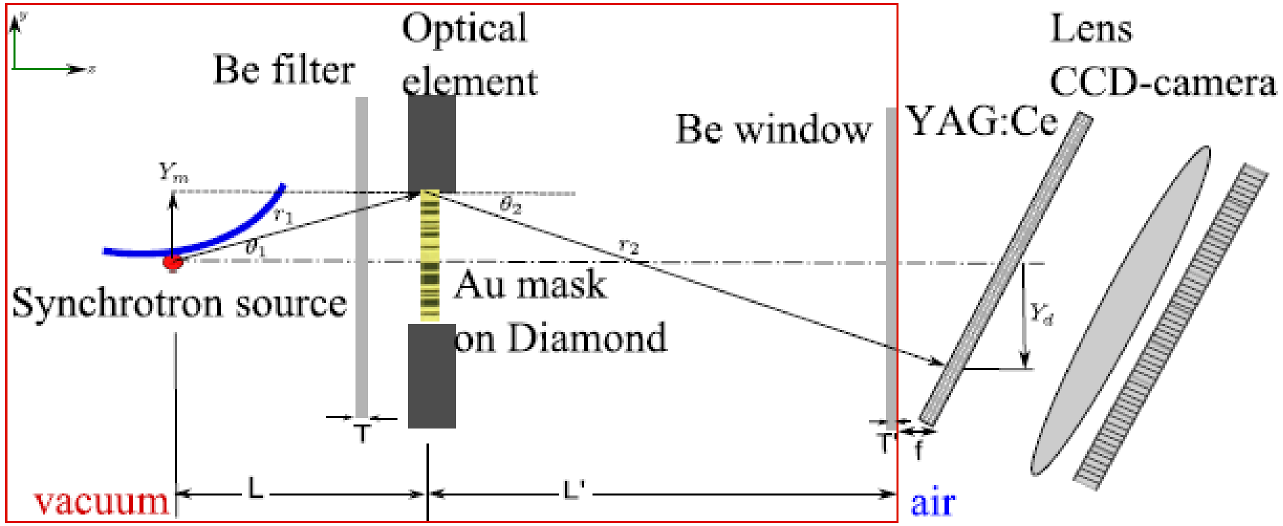

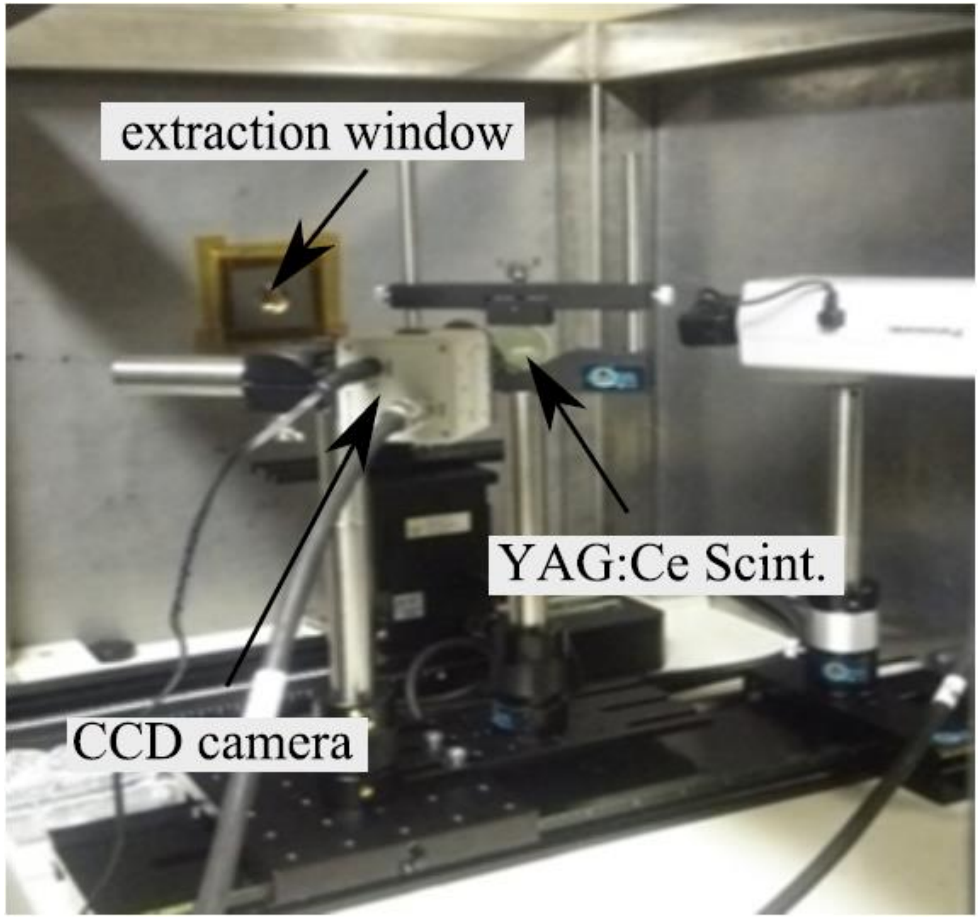

Figure 8: Schematic of XRM Beam Line. The beam passes through the Be filter, optical elements and Be window, and is then deposited in the 141 μm thick YAG scintillator.

(Note: LuAG in Phase II)

SuperKEKB X-ray Monitor: control room display panel

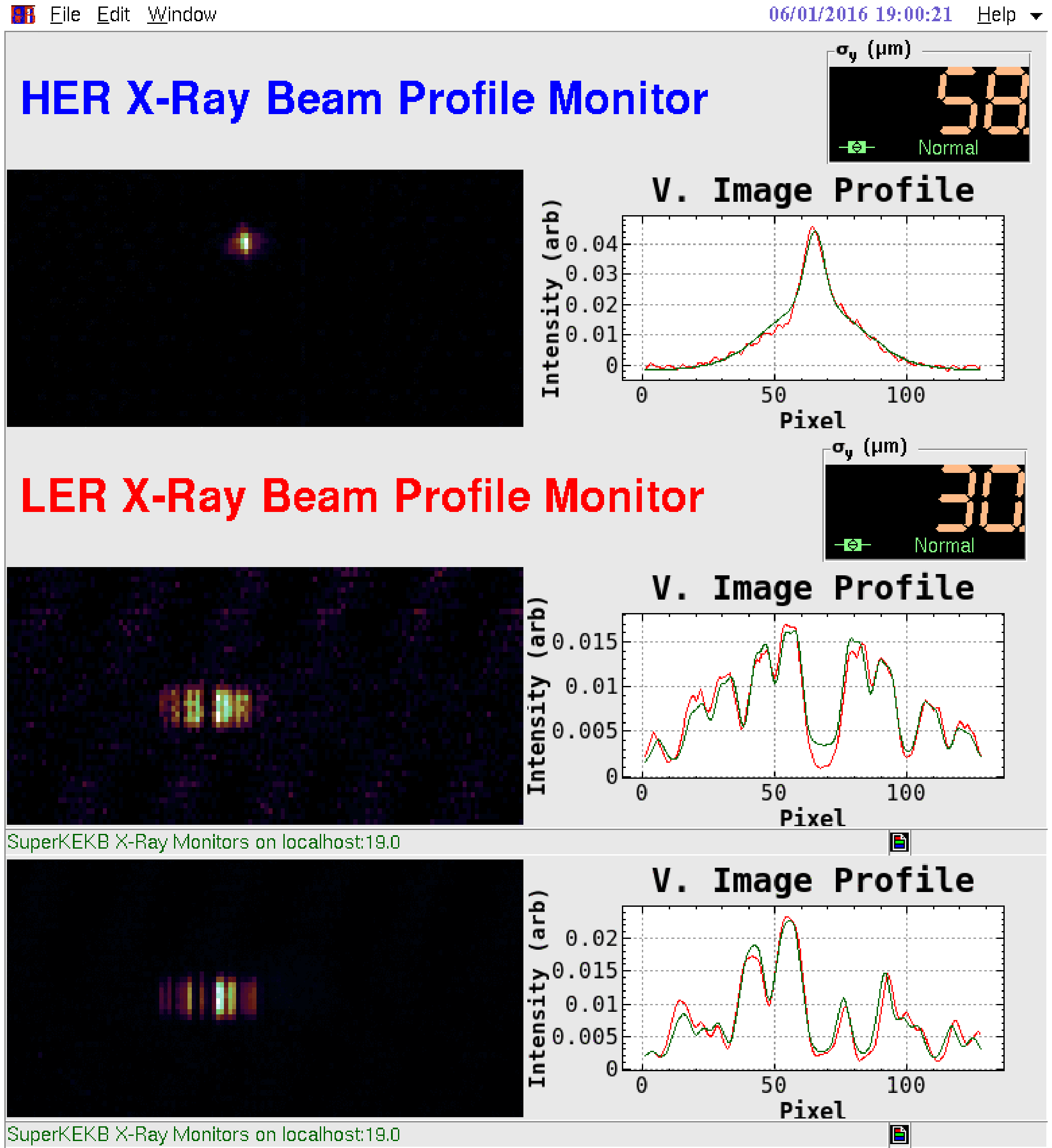

Phase I of SuperKEKB commissioning

Single-slit mask

Multi-slit mask

URA mask

SuperKEKB XRM: Status

- HER and LER beam lines commissioned, and taking data with scintillators.
- Template fits implemented for taking data with single-slit, multi-slit and URA masks.
- Calibration studies undertaken:
  - Source-point measurement
  - Overall magnification studies
    - Emittance Knob studies
    - Mask movement studies
    - Source-point movement studies
    - Changing beta function at source point (HER)
  - Light-level dependence (HER)
- Beam studies undertaken
  - Emittance measurements at LER and HER,
  - Electron cloud (LER) and current-dependence (HER)

SuperKEKB XRM: e-cloud blow-up study (LER)

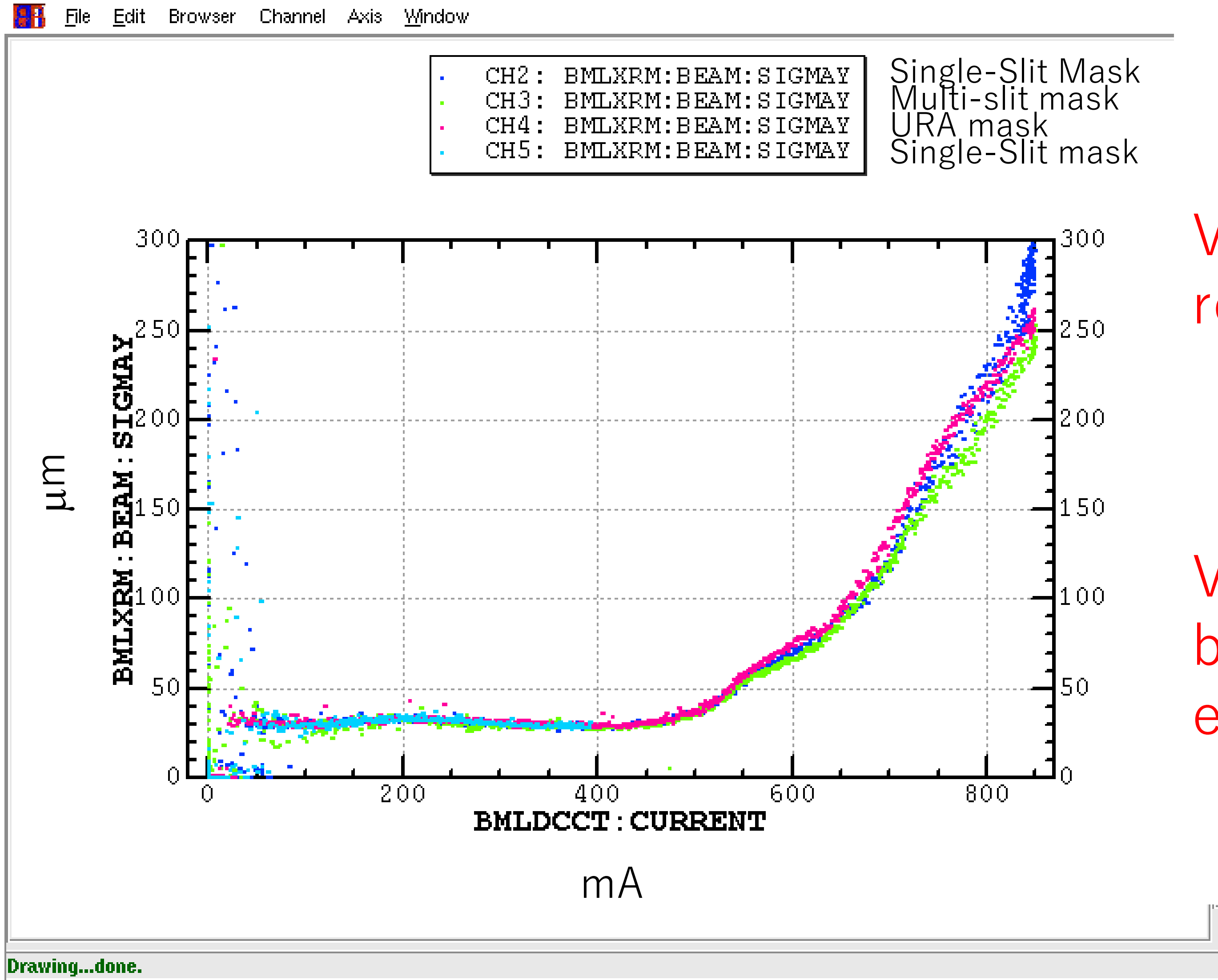

Very good fill-to-fill repeatability

Very good agreement between different masks, especially below 150 µm.

Experience at SuperKEKB

- Issues identified:
  - Suspected excessive scattering at Be filter in Phase I
    - Replaced Be filters with thinner ones for Phase II
    - Seems to have cured problem of excessive beam image point-spread function in HER
      - Now get point-spread function explainable by scintillator/camera system limitations
      - PSF small enough to measure minimum expected possible emittance in both HER and LER
  - Excessive ionization in air path
    - Filled detector box with helium for Phase II
      - Still some issues to work out with that
- Other:
  - Replaced scintillator cameras with higher-resolution versions during Phase II.
  - Added horizontal beam size measurement using knife-edge method with horizontal aperture edges.
  - Aim to start commissioning high-speed single-shot measurement system during Phase III.

Visible x-ray path in air (LER, 100 mA):

XRM display panel (Phase 2)

- Have measured **vertical beam sizes down to ~12 microns** using coded aperture (URA).
- Added **horizontal beam size measurement via knife-edge method** using horizontal aperture edges.
- Note: all measurements based on scintillator + camera. Single-shot measurements using Si detector planned for Phase 3 of SuperKEKB commissioning.

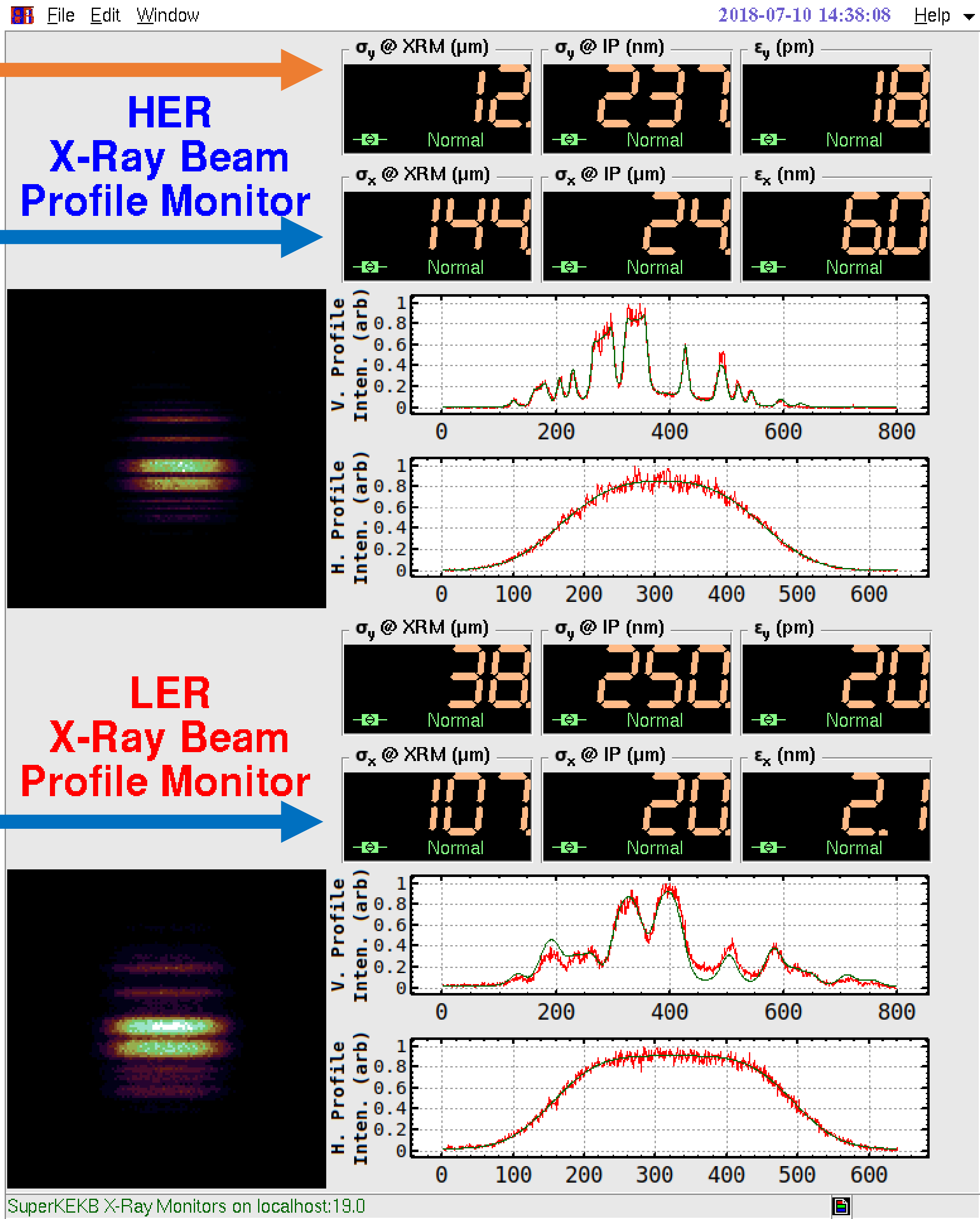

SuperKEKB Prospects

- Recall that I mentioned that template fitting works when basic source distribution is known, and characterized by a small number of parameters.
- For instability studies, such as electron-cloud-induced head-tail instabilities, the source distribution can become quite perverse. In fact, becoming non-Gaussian can itself be a diagnostic for the onset of certain instabilities. So it would be nice to be able to reconstruct the actual image of the beam.

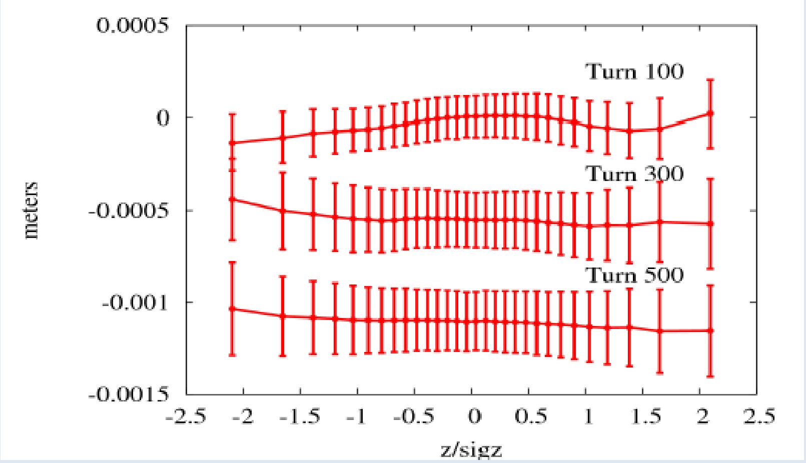

E-cloud induced head-tail motion simulation, adapted from E. Benedetto *et al*, PAC07, 4033 (2007)

- Which brings us back to the direct deconvolution reconstruction methods, which are being studied by E. Mulyani for use at SuperKEKB.
  - This would be especially useful for single-shot measurements, which are not averaged over many bunches and turns.
  - Direct reconstruction is much faster than template fitting, if potentially less accurate.
    - 2500 bunches * thousands of turns/bunch = a lot of data!

Direct reconstruction at SuperKEKB

- Preliminary results:
  - Beam images reconstructed from coded aperture data using Fourier transform and correlation methods.
  - Results fitted with a Gaussian.
  - Resulting beam sizes compared with template fit results.
- → Good agreement found between 40 and 80 μm beam sizes.
  - Slightly better agreement with template fits for correlation method than FT reconstruction.
  - Further study of systematics needed.

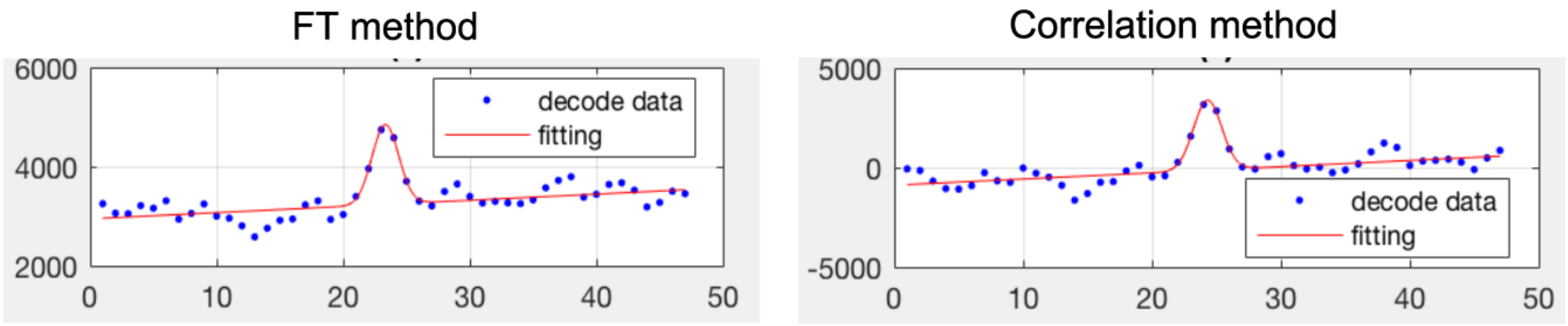

Image reconstruction process using (left) direct deconvolution/FT and (right) correlation methods.

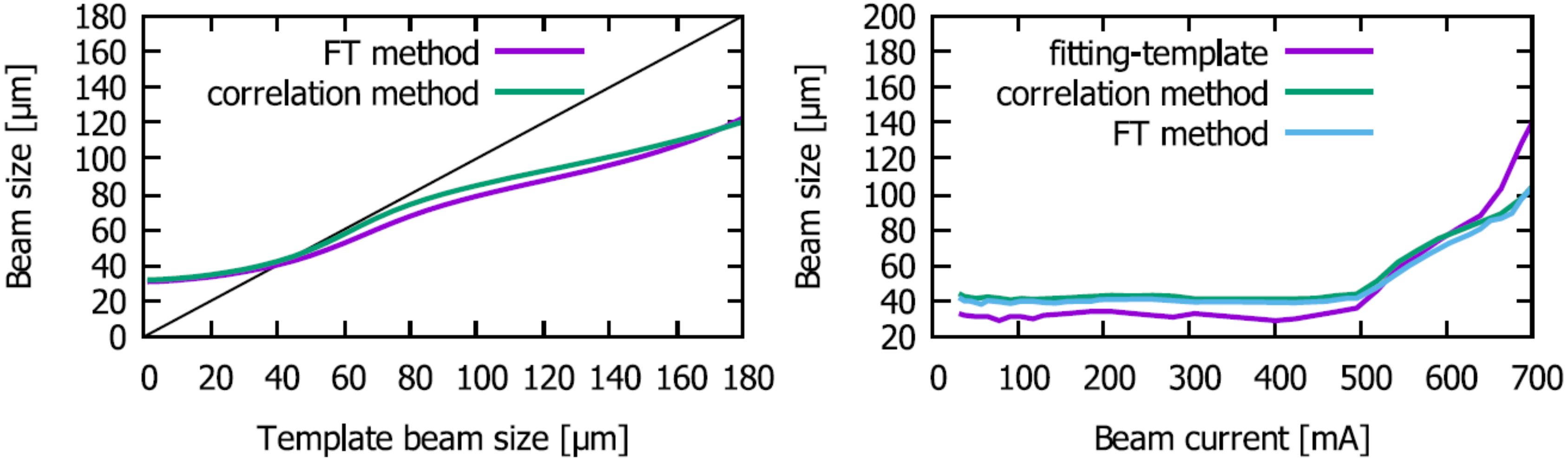

Comparison of CA deconvolution technique and template-fitting method.

E. Mulyani et al., "IMAGE RECONSTRUCTION TECHNIQUE BASED ON CODED APERTURE IMAGING FOR SuperKEKB X-RAY BEAM SIZE MONITOR," Proc. IPAC2018, Vancouver, Canada, JaCOW Publishing, May 2018 doi:10.18429/JACoW-IPAC2018-THPML074

Future plans re: fast reconstruction

- To eliminate side lobes in reconstruction (preserving delta function nature of A*G), really want either
  - Repeating mask pattern with detector large enough to image one full cycle, or;
  - Detector large enough to always contain projected image, even if image shifts due to beam position offset.
- Our current mask is single-cycle, and detector is only large enough to image one mask cycle.
  - Fine for template fitting, even if image goes partially off edge of detector, but:
  - For fast reconstruction, plan to make cyclic repeating mask pattern for next iteration of mask design.
    - Not much we can do about detector size in near term.
- Also plan further studies on reconstruction systematics and methods.

Ideal case for fast reconstruction

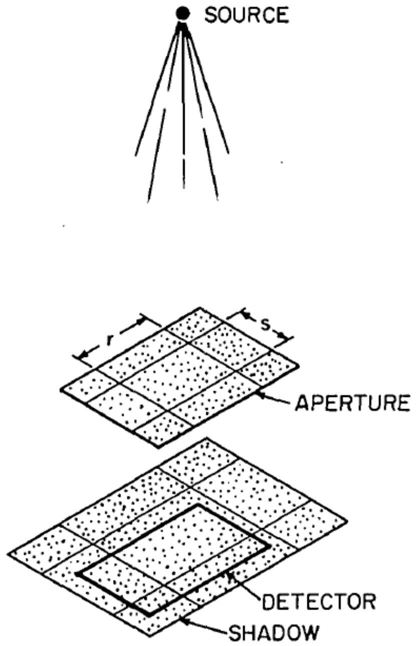

Fig. 3. This arrangement for a coded aperture imaging system employs a $2r$ by $2s$ aperture composed of a mosaic of basic r by s patterns. Emitting points in the source produce shadows of cyclic versions of the basic aperture pattern upon the detector, which need be only r by s in size.

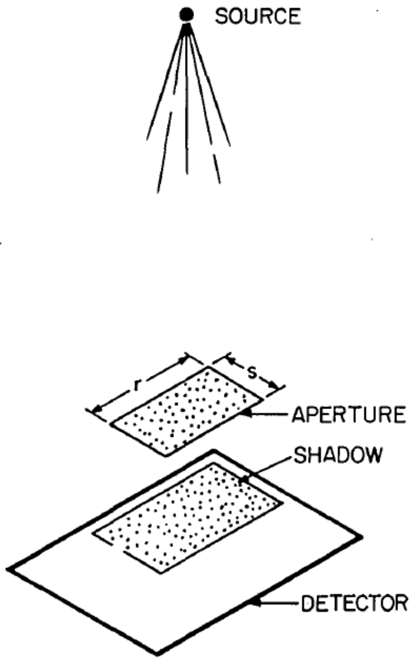

Fig. 4. This coded aperture arrangement employs only the basic r by s pattern for the aperture and has the disadvantage that the detector must be large enough to contain the image from the full field of view.

E.E. Fenimore and T.M. Cannon, Appl. Optics, V17, No. 3, p. 337 (1978).

Summary

- Coded aperture techniques have been tested for beam-size measurement at Diamond Light Source, CesrTA, ATF and SuperKEKB.
  - Using both URA and other mask patterns
- CA forms the primary beam size measurement system at SuperKEKB.
- Template fitting methods for measuring the beam size have been well demonstrated.
- Direct deconvolution is being tested for faster reconstruction at SuperKEKB.
  - Next iteration of mask design will be optimized for use with fast reconstruction techniques.

Thank you for listening!